Institute for Fundamental Theory Preprint UFIFT -HEP-91-22

DOE/ER/40272--138

DE92 008779

SDC

SOLENOIDAL DETECTOR NOTES

Jets in the Forward Region

R. D. Field

Institute for Fundamental Theory, Department of Physics
University of Florida, Gainesville, FL 32611

M. Barnett

Lawrence Berkeley Laboratory
University of California, Berkeley, CA 91125

A. White

Department of Physics, Box 19059
University of Texas at Arlington, Arlington, TX 76019

Abstract

We examine jet shapes in the forward region, $\eta(\text{jet}) > 4$, of 40 TeV proton-proton collisions and compare them with 90° jets. In the laboratory, forward jets are Lorentz contracted into thin "disks". For example, a jet which at $\theta_{cm}(\text{jet}) = 90°$ would have its particles located within a "cone" with angular widths $\Delta\theta_{cm} = \Delta\phi = 28°$ (i.e., 0.5 radians), if "boosted" to $\eta(\text{jet}) = 4$ ($\theta_{cm} = 2°$) becomes a "disk" with an angular width of $\Delta\theta_{cm} = 1°$! Jet shapes are roughly invariant when plotted versus pseudorapidity, η, and azimuthal angle, ϕ. In addition, we examine how well the electromagnetic component (i.e., *photons* and *electrons*) of a jet "tracks" the true position of the jet.

UFIFT-HEP-91-22
SDC-91-00043

SDC

SOLENOIDAL DETECTOR NOTES

Jets in the Forward Region

R. D. Field

Institute for Fundamental Theory, Department of Physics
University of Florida, Gainesville, FL 32611

M. Barnett

Lawrence Berkeley Laboratory
University of California, Berkeley, CA 91125

A. White

Department of Physics, Box 19059
University of Texas at Arlington, Arlington, TX 76019

Abstract

We examine jet shapes in the forward region, $\eta(\text{jet}) > 4$, of 40 TeV proton-proton collisions and compare them with 90° jets. In the laboratory, forward jets are Lorentz contracted into thin "disks". For example, a jet which at $\theta_{cm}(\text{jet}) = 90°$ would have its particles located within a "cone" with angular widths $\Delta\theta_{cm} = \Delta\phi = 28°$ (*i.e.*, 0.5 radians), if "boosted" to $\eta(\text{jet}) = 4$ ($\theta_{cm} = 2°$) becomes a "disk" with an angular width of $\Delta\theta_{cm} = 1°$! Jet shapes are roughly invariant when plotted versus pseudorapidity, η, and azimuthal angle, ϕ. In addition, we examine how well the electromagnetic component (*i.e.*, ***photons*** and ***electrons***) of a jet "tracks" the true position of the jet.

I. Introduction

There are two contrasting ways in which jets can be produced in the forward region in high-energy proton-proton collisions. Suppose that in 40 TeV collisions a jet with a transverse energy of 100 GeV is produced at a center-of-mass scattering angle, θ_{cm}(jet), of 2° ($\eta = 4$). . One way this can occur is for the parton-parton two-to-two subprocess, $a + b \rightarrow c + d$, to have its center of mass at rest in the laboratory (*i.e.*, $x_a \approx x_b$) with an outgoing parton energy of about 2.9 TeV. This process is suppressed because of the large parton-parton center-of- mass energy required ($\approx$ 5.7 TeV). The particles forming the outgoing jet would, on the average, be distributed within a "cone" centered along the jet direction. Cones containing 80% of the jet energy typically have a half-angle of about 30° so that jets arising in this manner would distribute their fragments over the entire forward region , $\theta_{cm} < 30°$.

A more economical way to produce a jet with transverse energy of 100 GeV at an angle of θ_{cm}(jet) = 2° is to produce, in the parton-parton center-of-mass frame, a 90° two-to-two hard scattering in which the outgoing parton has a transverse energy of 100 GeV, but with $x_a >> x_b$ (*i.e.*, in a frame "boosted" along the direction of the incident proton). In this case the parton-parton center-of-mass energy is only about 0.2 TeV. Since parton-parton cross sections decrease rapidity with center-of-mass energy forward jets are dominantly of this type. The shape of a "boosted" jet remains roughly invariant when plotted versus pseudorapidity, η. Momenta in the transverse direction are invariant under a Lorentz transformation so that the jet shape in the azimuthal angle ϕ is unaffected. Hence a jet which at θ_{cm}(jet) = 90° would have its particles located within the angular widths $\Delta\theta_{cm} = \Delta\phi \doteq 28°$ (*i.e.*, 0.5 radians), if "boosted" in the forward direction to η(jet) = 4 ($\theta_{cm} = 2°$) becomes a "disk" with an azimuthal width of $\Delta\phi = 28°$ and an angular width of $\Delta\theta_{cm} = 1°$!

In this report we examine the properties of jets produced in the forward region of 40 TeV proton- proton collisions and compare them with 90° jets. In addition, we will examine how well the electromagnetic component (*i.e.*, ***photons*** and ***electrons***) of a jet "tracks" the true position of the jet and study the effectiveness of constructing the trans-

Table 1. Generated sample of 10,000 "two-jet" QCD events in 40 TeV proton-proton collisions with the hard-scattering transverse momentum, $\hat{k}_T$, in the range $100 \leq \hat{k}_T \leq 500\,\text{GeV}$ and with no restriction on the pseudorapidity of the jets. N is the number of particles (with π^0 taken to be *stable*) and E_T is the global transverse energy.

Observable	*Value*
σ	1.2×10^{-2} mb
$< \hat{k}_T >$	136 GeV
$< N >$	527
$< E_T >$	560 GeV
$gg \rightarrow gg$	64%
$gq \rightarrow qg$	21%
$g\bar{q} \rightarrow \bar{q}g$	10%

verse energy of a "jet" from knowledge of the full jet energy (electromagnetic *and* hadronic) plus knowledge of the position of the electromagnetic component.

II. Event Generation

ISAJET is used to generate an initial sample of 10,000 "two-jet" QCD events in 40 TeV proton- proton collisions with the hard-scattering transverse momentum, $\hat{k}_T$, in the range $100 \leq \hat{k}_T \leq 500\,\text{GeV}$ and with no restriction on the pseudorapidity of the jets. Some of the properties of this initial sample are given in Table 1. The average number of particles produced is 527 (taking the π^0 as *stable*) with an average global transverse energy of 560 GeV. On the average, about 52% of the global transverse energy arises from the outgoing two jets with the remainder coming from the underlying event (*i.e.*, initial

state bremsstrahlung and breakup of the beam and target hadrons). At these energies and transverse momenta $gg \to gg$ is the dominate parton subprocess (64%).

The hard two-to-two parton-parton scattering produces two large transverse momentum outgoing partons which subsequently fragment into "jets", where we use the "theoretical" definition of a jet. In this report, "jet 1" is the collection of outgoing particles resulting from the fragmentation of the first outgoing parton (*i.e.*, parton 1) and of any additional partons that may have been produced by parton 1 during the parton shower process. Similarly, for "jet 2". Jets defined in this manner are not experimental observables. These "theoretical jets" are ideally what one strives to detect in an experiment, however, in an experiment no matter what jet definition one uses one can never be sure that one has included all the correct particles without including extra particles arising, for example, from initial state bremsstrahlung.

III. Jets at $\theta_{cm} = 90°$

The 20,000 "jets" are examined and a subsample of 503 events is found in which $85° \leq \theta_{cm}(\text{jet}) \leq 95°$. Some of the properties of these "90°-jets" are given in Table 2. These "jets" are dominantly gluon jets (86%). The average jet transverse energy is 145 GeV and the average jet multiplicity is 52 (remember these are "theoretical jets"). Jets at 90° are similar to e^+e^- jets and their fragments are, on the average, located in a cone of half-angle β_{cone} about the net jet direction. On the average, 80% of the jet multiplicity is located within a cone of half-angle $\beta_{cone}(80\%\ N) = 65°$. The energy of the "jet" is more localized, with 80% of the jet energy located, on the average, within a cone of half-angle $\beta_{cone}(80\%\ E) = 28°$. The cone containing 80% of the total energy of the "jet", on the average, contains 44% of the overall jet multiplicity (*i.e.*, 44% of the particles carry, on the average, 80% of the energy).

Averages do not tell the whole story, however, as there are large fluctuations in QCD. This is reflected in the large standard deviations in Table 2. There is much more information in the distribution of cone sizes shown in Figs. 1 and 2. Fig. 1 shows the probability that 80% of particles from a given "jet" will be located within a cone of half-angle β_{cone}

Table 2. Selected sample of 503 "90°-jets" (*i.e.*, $85 \leq \theta_{cm}(\text{jet}) \leq 95°$) from the 20,000 "jets" generated in Table 1. We have used the "theoretical" definition of a jet (*i.e.*, all the particles resulting from the fragmentation of an initial outgoing parton) and the ± signs correspond not to errors, but to the standard deviations from the mean.

Observable	*Value*
$< N(\text{jet}) >$	52
$< E_T(\text{jet}) >$	145 GeV
gluon-jet	86%
q-jet	7%
$\bar{q}$-jet	7%
$< \beta_{cone}(80\%\ N) >$	65° (1.13 radians)
$< \beta_{cone}(80\%\ E) >$	28° (0.49 radians)
f_{cone}	0.44
$< d_\eta(80\%\ N) >$	0.71 ± 0.30
$< d_\eta(80\%\ E_T) >$	0.27 ± 0.21
f_η	0.46
$< d_\phi(80\%\ N) >$	0.92 ± 0.43
$< d_\phi(80\%\ E_T) >$	0.30 ± 0.28
f_ϕ	0.44
$< R(80\%\ N) >$	1.29 ± 0.49
$< R(80\%\ E_T) >$	0.45 ± 0.35
f_R	0.41

and Fig. 2 shows the probability that 80% of jet energy will be located within a cone of

half-angle β_{cone}. One sees that although the average cone half-angle containing 80% of the energy is 28° about 21% of the "jets" have 80% of their energy contained within a cone with a half-angle of less than 9°! On the other hand, about 8% of the "jets" have 80% of their energy contained within a cone with a half-angle of greater than 63°. Fig. 3 gives the percentage of "90°-jets" which have a fraction, f_{cone}, of their total multiplicity located within the cone of half-angle β_{cone} about the jet direction which contains 80% of the jet energy.

Alternatively, one can describe the "size" of these "90°-jets" in terms of the pseudorapidity, η, and azimuthal angle, ϕ. Figs. 4 and 5 show the multiplicity flow and the transverse energy flow relative to the "jet" direction, respectively, versus pseudorapidity, $\eta - \eta(\text{jet})$, averaged over all "90°-jets". Similarly, Figs. 6 and 7 show the multiplicity flow and the transverse energy flow versus the azimuthal angle, ϕ, (where the events have been rotated so the $\phi(\text{jet}) = 180°$) again averaged over all "90°-jets". Table 2 shows that, on the average, 80% of the jet multiplicity is located within the "half-width" $d_\eta = 0.71$ of the jet direction (integrated over ϕ), where

$$d_\eta = |\eta - \eta(\text{jet})|,$$

and 80% of the jet transverse energy is located, on the average, within $d_\eta = 0.27$ of the jet direction (*i.e.*, an "average jet" is about 0.54 units "wide" when projected on the pseudorapidity axis). In addition, Table 2 shows that, on the average, 80% of the jet multiplicity is located within the "half-width" $d_\phi = 0.92$ (in radians) of the jet direction (integrated over η), where

$$d_\phi = |\phi - \phi(\text{jet})|,$$

and 80% of the jet transverse energy is located, on the average, within $d_\phi = 0.30$ of the jet direction (*i.e.*, an "average jet" is about 0.6 radians or 34° "wide" when projected on the ϕ-axis).

At 90° the reason that the jet size in pseudorapidity, d_η, and the jet size in azimuthal angle, d_ϕ, are nearly the same. This is simply a result of the cone structure of an average

jet at 90% and the definition of pseudorapidity. For example, suppose that a cone of half-angle β_{cone} is located with its axis at 90°. In this case,

$$d_\phi = \beta_{cone},$$

and

$$\theta_{cm} = 90^\circ - \beta_{cone},$$

so that

$$\begin{aligned}\eta &= -\log\left(\tan(\theta_{cm}/2)\right) \\ &= -\log\left(\tan(45^\circ - \beta_{cone}/2)\right) \\ &= -\log\left(\frac{1-\tan(\beta_{cone}/2}{1+\tan(\beta_{cone}/2}\right),\end{aligned}$$

or

$$e^{-\eta} = \frac{1-\tan(\beta_{cone}/2)}{1+\tan(\beta_{cone}/2)}.$$

For small η the left hand side becomes

$$e^{-\eta} \approx 1 - \eta + \frac{1}{2}\eta^2 - \cdots,$$

while for small β_{cone} the left hand side is

$$\frac{1-\frac{1}{2}\beta_{cone}+\cdots}{1+\frac{1}{2}\beta_{cone}-\cdots} \approx 1 - \beta_{cone},$$

and hence

$$\eta \approx \beta_{cone} \qquad (\text{for } \beta_{cone} << 1 \text{ radian}).$$

Fig. 8 shows that if $\beta_{cone} < 45^\circ$ then for a 90° cone β_{cone} in radians is very closely equal to the pseudorapidity η. In Table 2, $< d_\phi(80\%\ E_T) >= 0.3$ (*i.e.*, about 17°) hence is almost equal to $< d_\eta(80\%\ E_T) >$. On the other hand, $< d_\phi(80\%\ N) >= 0.92$ (*i.e.*, about 53°) and does not agree as well with $< d_\eta(80\%\ N) >$.

As before, averages (*i.e.*, sums of all events) do not show the fluctuations of QCD. More information is contained in the event-by-event (*i.e.*, jet-by-jet) distributions of the "half-widths" d_η and d_ϕ. Figs. 9 and 10 shows the percentage of "jets" for which 80% of the multiplicity and 80% of the transverse energy, respectively, is contained with a half-width, d_η. Similarly, Figs. 11 and 12 shows the percentage of "jets" for which 80% of the

multiplicity and 80% of the transverse energy, respectively, is contained with a half-width, d_ϕ. Fig. 10 shows that although $< d_\eta(80\%\ E_T) >= 0.27$, about 24% of the jets have 80% of their transverse energy contained with a half-width of $d_\eta(80\%\ E_T) = 0.1$. This is sometimes referred to a "hot jet core". On the other hand, this figure also shows that for about 9% of the "jets" 80% of their transverse energy is contained with a half-width of $d_\eta(80\%\ E_T) > 0.6$. Some "jets" are "fat" and some are "skinny".

Instead of projecting the jet size on the pseudorapidity or the azimuthal angle axis, one can describe the size of a jet with one parameter. The cone angle β_{cone} was used to describe 90° jets. However, as we will see the particles resulting from jets in the forward region (*i.e.*, θ_{cm} small) do not, on the average, lie in a cone. Another variable that can be used to describe the size of a jets is the "radius", R, in η-ϕ space. Namely,

$$R = \sqrt{d_\eta^2 + d_\phi^2},$$

where $d_\eta = |\eta - \eta(\text{jet})|$ and $d_\phi = |\phi - \phi(\text{jet})|$ and where d_ϕ is measured in radians.. Table 2 shows that, on the average, 80% of the multiplicity and transverse energy of a "jet" is contained within a "radius" R of 1.29 and 0.45, respectively. An "average jet" contains 80% of its transverse energy with a "radius" of about 0.5 (with about 40% of the jet multiplicity within this radius).

Of course, fluctuations are very prevalent. Figs. 13 and 14 show the percentage of "jets" for which 80% of the multiplicity and 80% of the transverse energy, respectively, are contained within the "radius" R. At 90° about 14% of the "jets" have 80% of their transverse energy contained within a "radius" of 0.1, while for 10% of the "jets" one needs a "radius" greater than 1.0!

IV. Jets in the Forward Region

Jets in the forward region (*i.e.*, $\eta(\text{jet}) > 4$) arise from two-to-two subprocess in which the parton-parton center of mass is "boosted" along the incident proton direction (*i.e.*, along the $\hat{z}$- axis). Because of the Lorentz contraction "jets" no longer appear, on the average, as cones. The shape in the azimuthal angle ϕ remains roughly invariant, while the

Table 3. Angular size (in degrees) of a pseudorapidity bin of size $\Delta\eta = 0.5$ centered at a pseudorapidity η_{center}.

η_{center}	θ_{cm}(center)	$\Delta\theta_{cm}$
0.0	90°	28.35°
1.0	40.4°	18.59°
2.0	15.4°	7.68°
3.0	5.7°	2.87°
4.0	2.1°	1.06°
5.0	0.77°	0.39°
6.0	0.28°	0.14°

shape in θ_{cm} is compressed. If we were using the true rapidity rather than pseudorapidity, the size would remain invariant. Shapes in pseudorapidity remain roughly invariant except for slow particles where mass effects become important. This means that jets in the forward region look, in the laboratory, more like sections of a "disk". Using Table 3 one can see that a 90° jet with a "radius" $R = 0.5$ when "boosted" in the forward region to $\eta(\text{jet}) = 4$ ($\theta_{cm} = 2°$) becomes a "disk" with an azimuthal width of $\Delta\phi = 28°$ and an angular width of $\Delta\theta_{cm} = 1°$!

Figs. 15 and 16 show the multiplicity flow and transverse energy flow of a single "jet" that originated from a parton with $\eta(\text{parton}) = 5.15$ (*i.e.*, 0.66°) and $\phi(\text{parton}) = 180°$, respectively, versus pseudorapidity, while Figs. 17 and 18 show the multiplicity flow and transverse energy flow, respectively, versus the center of mass angle, θ_{cm}. All the transverse energy is located in an angular region $\Delta\theta_{cm}$ of less that one degree. Figs. 19 and 20 show the multiplicity flow and transverse energy flow, respectively, versus the azimuthal angle ϕ. Here the width is similar to a 90° jet.

From the generated 20,000 "jets" 437 "forward jets" are selected ($4 < \eta(\text{jet}) < 6.5$)

Table 4. Selected sample of 437 "forward-jets" (*i.e.*, $\eta(\text{jet}) > 4$) from the 20,000 "jets" generated in Table 1. We have used the "theoretical" definition of a jet (*i.e.*, all the particles resulting from the fragmentation of an initial outgoing parton) and the $\pm$ signs correspond not to errors, but to the standard deviations from the mean.

Observable	*Value*
$< N(\text{jet}) >$	55
$< E_T(\text{jet}) >$	124 GeV
gluon-jet	47%
q-jet	37%
$\bar{q}$-jet	16%
$< d_\eta(80\%\ N) >$	0.96 ± 0.54
$< d_\eta(80\%\ E_T) >$	0.43 ± 0.45
f_η	0.48
$< d_\phi(80\%\ N) >$	1.15 ± 0.52
$< d_\phi(80\%\ E_T) >$	0.40 ± 0.42
f_ϕ	0.45
$< R(80\%\ N) >$	1.61 ± 0.67
$< R(80\%\ E_T) >$	0.66 ± 0.59
f_R	0.42

and analyzed. Table 4 show some of the properties of the "forward jets". The flavor of these jets is somewhat different than the 90° sample (there is a higher percentage of quark jets). The forward jets are a little "fatter" on the average, however this is not a big effect. In the forward region $< R(80\%\ E_T) >= 0.66$ while at 90° one has 0.45. Figs. 9 and 10 compare the pseudorapidity half-widths $d_\eta(80\%\ N)$ and $d_\eta(80\%\ E_T)$ for

the forward jets with the 90° jets and Figs. 11 and 12 compares the azimuthal angle half-widths $d_\phi(80\%\ N)$ and $d_\phi(80\%\ E_T)$ for the forward jets with the 90° jets. In both cases the forward jets are a bit broader, but the differences are small. Similarly, Figs. 13 and 14 compare the "radius" R containing 80% of the "jet" multiplicity and transverse energy, respectively, for the forward jets with the 90° jets. Again the differences are small., however, the forward region contains more fat jets. About 20% of the forward jets have 80% of their transverse energy contained in a radius greater than 1.0 compared to only 10% of the 90° jets.

V. The Electromagnetic Component of a Jet

We would like to find out how the electromagnetic component (*i.e.*, *photons* and *electrons*) of a jet "tracks" the position of the jet. A sample of 2,000 jets from the first 1,000 events in Table 1 are analyzed but with the π^0 allowed to decay into photons. Some properties of these events are shown in Table 5. The particle multiplicity has increased because of the photons otherwise the events are very similar to those in Table 1 and Table 2. Fig. 21 shows the percentage of "jets" for which the electromagnetic component carries a fraction, f_1 (f_2), of the total jet energy (transverse energy). For an average "jet" $E_T^{em}(\text{jet})/E_T(\text{jet}) = 0.24$, however, there are large fluctuations as can be seen. Fig. 22 illustrates how well the electromagnetic component of a jets tracks the position of the jet in pseudorapidity and azimuthal angle, respectively. Fig. 23 gives the percentage of "jets" for which the electromagnetic component is located a "distance", d_{em}, in η-ϕ space away from the true jet position. In particular,

$$d_{em} = \sqrt{(\eta(\text{em}) - \eta(\text{jet}))^2 + (\phi(\text{em}) - \phi(\text{jet}))^2},$$

where $\eta(\text{em})$ and $\phi(\text{em})$ are the positions of the electromagnetic component of the jet. As can be seen from Table 5, on the average, d_{em} is about 0.17. Again, however, there are large fluctuations. Fig. 23 shows that about 27% of the "jets" had d_{em} less than 0.05 and about 10% of the "jets" have d_{em} greater than 0.3!

It is interesting to see how well one can reconstruct the transverse energy of a jet using only the electromagnetic component to determine the position (*i.e.*, θ_{em}). Fig. 24 shows

Table 5. Generated sample of 1,000 "two-jet" QCD events in 40 TeV proton-proton collisions. N is the number of particles (with the π^0 allowed to decay). E_{em}(jet) and E_T^{em}(jet) are the electromagnetic (*i.e.*, *photons* and *electrons*) energy and transverse energy, respectively, of the "jet". Similarly, η(em) and ϕ(em) are the positions of the electromagnetic component of the jet and $d_{em} = \sqrt{(\eta(\text{em}) - \eta(\text{jet}))^2 + (\phi(\text{em}) - \phi(\text{jet}))^2}$. The constructed jet transverse energy, E_T(con), is computed using the only the electromagnetic component to give the direction and then assigning the total energy of the jet (electromagnetic *and* hadronic) to be in that direction.

Observable	*Value*
$< N >$	663
$< N(\text{jet}) >$	68
$< E_T(\text{jet}) >$	142 GeV
$< E_{em}(\text{jet})/E(\text{jet}) >$	0.24 ± 0.14
$< E_T^{em}(\text{jet})/E_T(\text{jet}) >$	0.24 ± 0.14
$< \eta(\text{em}) - \eta(\text{jet}) >$	0.00 ± 0.20
$< \phi(\text{em}) - \phi(\text{jet}) >$	0.00 ± 0.19
$< E_T(\text{con})/E_T(\text{jet}) >$	0.95 ± 0.14
$< d_{em} >$	0.17 ± 0.22

the ratio of the constructed jet transverse energy, E_T(con), to the true jet transverse energy, where

$$E_T(\text{con}) = E(\text{jet}) \ \sin\theta_{em}.$$

Table 6. Selected sample of 467 forward (*i.e.*, $\eta(\text{jet}) > 4$) "jets" in 40 TeV proton-proton collisions. N is the number of particles (with the π^0 allowed to decay). $E_{em}(\text{jet})$ and $E_T^{em}(\text{jet})$ are the electromagnetic energy (*i.e.*, *photons* and *electrons*) and transverse energy, respectively, of the "jet". Similarly, $\eta(\text{em})$ and $\phi(\text{em})$ are the pseudorapidity and azimuthal angle of the electromagnetic component of the jet. The constructed jet transverse energy, $E_T(\text{con})$, is computed using the only the electromagnetic component to give the direction and then assigning the total energy of the jet (electromagnetic *and* hadronic) to be in that direction.

Observable	*Value*
$< N(\text{jet}) >$	69
$< E_T(\text{jet}) >$	126 GeV
$< E_{em}(\text{jet})/E(\text{jet}) >$	0.24 ± 0.15
$< E_T^{em}(\text{jet})/E_T(\text{jet}) >$	0.23 ± 0.14
$< \eta(\text{em}) - \eta(\text{jet}) >$	0.00 ± 0.19
$< \phi(\text{em}) - \phi(\text{jet}) >$	0.00 ± 0.22
$< E_T(\text{con})/E_T(\text{jet}) >$	0.89 ± 0.16

Here we assume complete (*i.e.*, *exact*) knowledge of the jet energy (sum of electromagnetic ***and*** hadronic), but the information as to the position of the jet comes solely from the electromagnetic part. In particular, we assume exact knowledge of the position and energy of the electromagnetic component of the jet and exact knowledge of the energy of the hadronic component, but assume no knowledge as to the position of the hadronic component. On the average, this does not work badly (the average ratio from Table 5

is 0.95). The fluctuations, however, probably make this method of "jet" reconstruction useless. For example, Fig. 24 shows that about 15% of the time one underestimates the jet transverse energy by more that 20%.

For forward jets, $\eta(\text{jet}) > 4$, the situation is similar. Table 6 gives some properties of a selected sample of 467 forward "jets" in proton-proton collisions at the SSC center of mass energy of 40 TeV with the hard scattering transverse momentum, $\hat{k}_T$, in the range $100 \leq \hat{k}_T \leq 500\,\text{GeV}$ (with the π^0 allowed to decay). Fig. 25 shows how well the electromagnetic component of a jets tracks the position of the jet in pseudorapidity and azimuthal angle, respectively, for forward jets. The plot is similar to the 90° jets in Fig. 22. Fig. 26 shows the ratio of the constructed jet transverse energy, $E_T(\text{con})$, to the true jet transverse energy for forward jets. Again the results are similar to the 90° case.

Figure Captions

Fig. 1. Percentage of "90°-jets" for which 80% of the jet multiplicity is located within a cone of half-angle β_{cone} (in degrees) about the jet direction. Included in the plot are the 503 jets whose properties are listed in Table 2. The average "jet" contains 52 particles and has a transverse energy of 145 GeV.

Fig. 2. Percentage of "90°-jets" for which 80% of the jet energy is carried by particles located within a cone of half-angle β_{cone} (in degrees) about the jet direction. Included in the plot are the 503 jets whose properties are listed in Table 2.

Fig. 3. Percentage of "90°-jets" which have a fraction, f_{cone}, of their total multiplicity located within the cone of half-angle β_{cone} about the jet direction which contains 80% of the jet energy. Included in the plot are the 503 jets whose properties are listed in Table 2.

Fig. 4. Multiplicity flow about the jet direction projected on the pseudorapidity axis (integrated over all azimuthal angles ϕ). Included in the plot are the 503 "90°-jets" whose properties are listed in Table 2 and the 437 "forward jets" whose properties are given in Table 4.

Fig. 5. Transverse energy flow about the jet direction projected on the pseudorapidity axis (integrated over all azimuthal angles ϕ). Included in the plot are the 503 "90°-jets" whose properties are listed in Table 2 and the 437 "forward jets" whose properties are given in Table 4.

Fig. 6. Multiplicity flow about the jet direction (ϕ(jet) = 180°) projected on the azimuthal angle axis, ϕ (integrated over all pseudorapidity). Included in the plot are the 503 "90°-jets" whose properties are listed in Table 2 and the 437 "forward jets" whose properties are given in Table 4.

Fig. 7. Transverse energy flow about the jet direction (ϕ(jet) = 180°) projected on the

azimuthal angle axis, ϕ (integrated over all pseudorapidity). Included in the plot are the 503 "90°-jets" whose properties are listed in Table 2 and the 437 "forward jets" whose properties are given in Table 4.

Fig. 8. Plot of the pseudorapidity, η, versus the angle β (in degrees), where the center of mass angle $\theta_{cm} = 90° - \beta$ and the pseudorapidity is given by $\eta = -\log(\tan(\theta_{cm}/2))$. Also plotted is the angle β in radians versus β in degrees. For β small β(in radians) $\approx \eta$.

Fig. 9. Percentage of "jets" for which 80% of the jet multiplicity is located within a half-width, $d_\eta = |\eta - \eta(\text{jet})|$, in pseudorapidity (integrated over all azimuthal angle ϕ) about the jet direction. Included in the plot are the 503 "90°-jets" whose properties are listed in Table 2 and the 437 "forward jets" whose properties are given in Table 4.

Fig. 10. Percentage of "jets" for which 80% of the jet transverse energy is carried by particles located within a half-width, $d_\eta = |\eta - \eta(\text{jet})|$, in pseudorapidity (integrated over all azimuthal angle ϕ) about the jet direction. Included in the plot are the 503 "90°- jets" whose properties are listed in Table 2 and the 437 "forward jets" whose properties are given in Table 4.

Fig. 11. Percentage of "jets" for which 80% of the jet multiplicity is located within a half-width, $d_\phi = |\phi - \phi(\text{jet})|$, in azimuthal angle (integrated over all pseudorapidity) about the jet direction. Included in the plot are the 503 "90°-jets" whose properties are listed in Table 2 and the 437 "forward jets" whose properties are given in Table 4.

Fig. 12. Percentage of "jets" for which 80% of the jet transverse energy is carried by particles located within a half-width,$d_\phi = |\phi - \phi(\text{jet})|$, in azimuthal angle (integrated over all pseudorapidity) about the jet direction. Included in the plot are the 503 "90°-jets" whose properties are listed in Table 2 and the 437 "forward jets" whose properties are given in Table 4.

Fig. 13. Percentage of jets for which 80% of the jet multiplicity is located within a radius,

$R = \sqrt{d_\eta^2 + d_\phi^2}$, about the jet direction. Included in the plot are the 503 "90°-jets" whose properties are listed in Table 2 and the 437 "forward jets" whose properties are given in Table 4.

Fig. 14. Percentage of jets for which 80% of the jet transverse energy is carried by particles located within a radius, $R = \sqrt{d_\eta^2 + d_\phi^2}$, about the jet direction. Included in the plot are the 503 "90°-jets" whose properties are listed in Table 2 and the 437 "forward jets" whose properties are given in Table 4.

Fig. 15. Multiplicity flow about the jet direction projected on the pseudorapidity axis (integrated over all azimuthal angles ϕ) for a single jet initiated by a "parent" parton with a pseudorapidity $\eta(\text{parton}) = 5.15$ (*i.e.*, 0.66°) and an azimuthal angle $\phi(\text{parton}) = 180°$. The jet has a transverse energy of 111 GeV and a particle multiplicity of 50.

Fig. 16. Transverse energy flow about the jet direction projected on the pseudorapidity axis (integrated over all azimuthal angles ϕ) for a single jet initiated by a "parent" parton with a pseudorapidity $\eta(\text{parton}) = 5.15$ (*i.e.*, 0.66°) and an azimuthal angle $\phi(\text{parton}) = 180°$. The jet has a transverse energy of 111 GeV and a particle multiplicity of 50.

Fig. 17. Multiplicity flow projected on the θ_{cm}-axis (integrated over all azimuthal angles ϕ) for a single jet initiated by a "parent" parton with $\theta_{cm}(\text{parton}) = 0.66°$ (*i.e.*, $\eta(\text{parton}) = 5.15$) and an azimuthal angle $\phi(\text{parton}) = 180°$. The jet has a transverse energy of 111 GeV and a particle multiplicity of 50.

Fig. 18. Transverse energy flow projected on the θ_{cm}-axis (integrated over all azimuthal angles ϕ) for a single jet initiated by a "parent" parton with $\theta_{cm}(\text{parton}) = 0.66°$ (*i.e.*, $\eta(\text{parton}) = 5.15$) and an azimuthal angle $\phi(\text{parton}) = 180°$. The jet has a transverse energy of 111 GeV and a particle multiplicity of 50.

Fig. 19. Multiplicity flow projected on the ϕ-axis (integrated over all pseudorapidity) for a

single jet initiated by a "parent" parton with $\theta_{cm}(\text{parton}) = 0.66°$ (*i.e.*, $\eta(\text{parton}) = 5.15$) and an azimuthal angle $\phi(\text{parton}) = 180°$. The jet has a transverse energy of 111 GeV and a particle multiplicity of 50.

Fig. 20. Transverse energy flow projected on the ϕ-axis (integrated over all pseudorapidity) for a single jet initiated by a "parent" parton with $\theta_{cm}(\text{parton}) = 0.66°$ (*i.e.*, $\eta(\text{parton}) = 5.15$) and an azimuthal angle $\phi(\text{parton}) = 180°$. The jet has a transverse energy of 111 GeV and a particle multiplicity of 50.

Fig. 21. Percentage of "jets" which have a fraction, $f_1 = E_{em}/E(\text{jet})$, of their total energy resulting from electromagnetic particles (*i.e.*, *photons* and *electrons*) and the percentage of "jets" which have a fraction, $f_2 = E_T^{em}/E_T(\text{jet})$, of their total transverse energy resulting from electromagnetic particles. The plot comes from the sample of 2,000 "jets" whose properties are given in Table 5.

Fig. 22. Compares the true position of a "jet" in pseudorapidity, η, and in azimuthal angle, ϕ, respectively with the position arrived at by taking only the electromagnetic particles (*i.e.*, photons and electrons) within the jet. The plot comes from the sample of 2,000 "jets" whose properties are given in Table 5.

Fig. 23. The "distance", $d = \sqrt{d_\eta^2 + d_\phi^2}$, between the true jet direction and the direction of the electromagnetic component of the jet (*i.e.*, *photons* and *electrons*). The plot shows the percentage of jets for which the direction electromagnetic component differs from the true direction by a distance, d. The plot comes from the sample of 2,000 "jets" whose properties are given in Table 5.

Fig. 24. Ratio of the transverse energy constructed using the direction of the electromagnetic component (*i.e.*, *photons* and *electrons*) of the jet to the true jet transverse energy, $E_T(\text{true})$. The constructed jet transverse energy, $E_T(\text{con})$, is computed using the only the electromagnetic component to give the direction and then assigning the total energy

of the jet (electromagnetic *and* hadronic) to be in that direction. The plot comes from the sample of 2,000 "jets" whose properties are given in Table 5.

Fig. 25. Compares the true position of a "jet" in pseudorapidity, η, and in azimuthal angle, ϕ, respectively with the position arrived at by taking only the electromagnetic particles (*i.e., photons* and *electrons*) within the jet. The plot contains the sample of 467 forward "jets" in Table 6.

Fig. 26. Ratio of the transverse energy constructed using the direction of the electromagnetic component (*i.e.*, photons and electrons) of the jet to the true jet transverse energy, $E_T(true)$. The constructed jet transverse energy, $E_T(\mathrm{con})$, is computed using the only the electromagnetic component to give the direction and then assigning the total energy of the jet (electromagnetic *and* hadronic) to be in that direction. The plot contains the sample of 467 forward "jets" in Table 6.

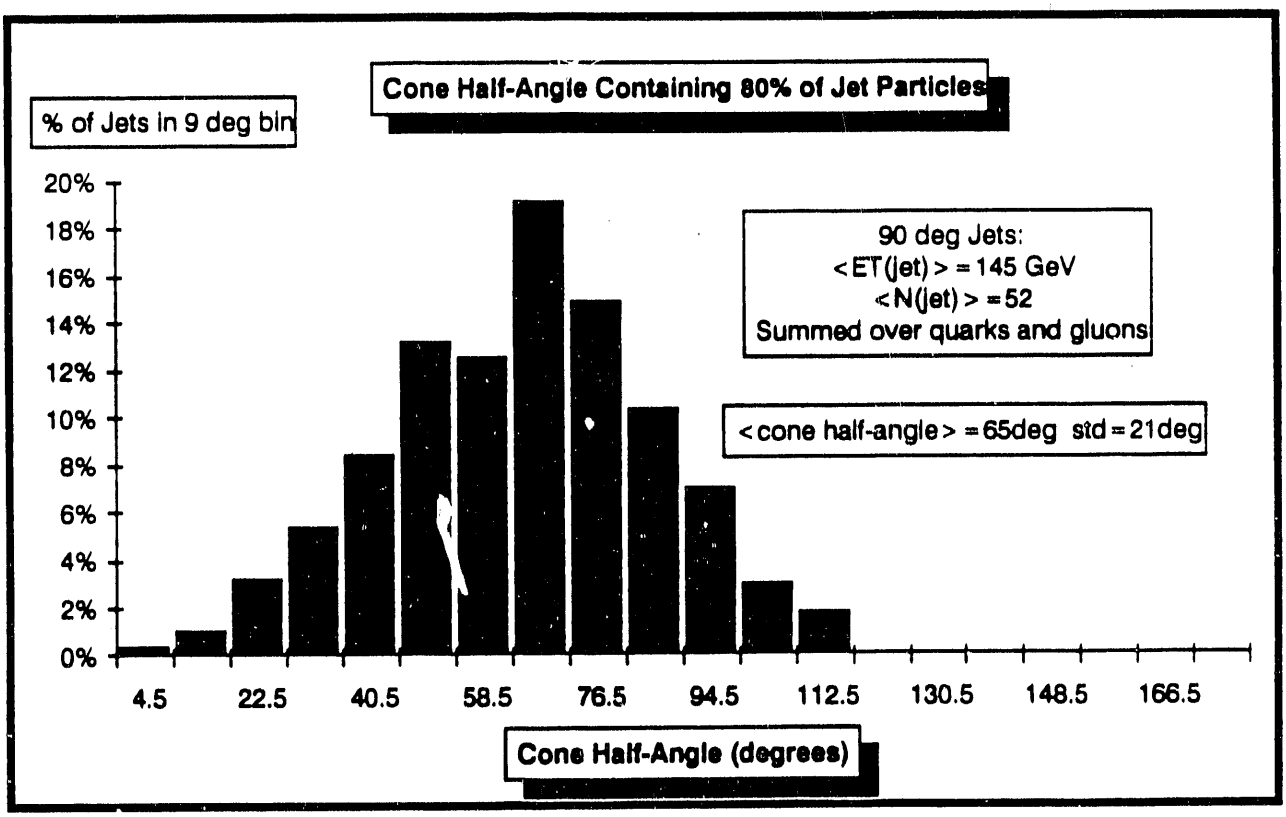
Cone Half-Angle Containing 80% of Jet Particles
% of Jets in 9 deg bin
20%
18%
16%
14%
12%
10%
8%
6%
4%
2%
0%
90 deg Jets:
<ET(jet)> = 145 GeV
<N(jet)> = 52
Summed over quarks and gluons
<cone half-angle> = 65deg std = 21deg
4.5
22.5
40.5
58.5
76.5
94.5
112.5
130.5
148.5
166.5
Cone Half-Angle (degrees)

Figure 1

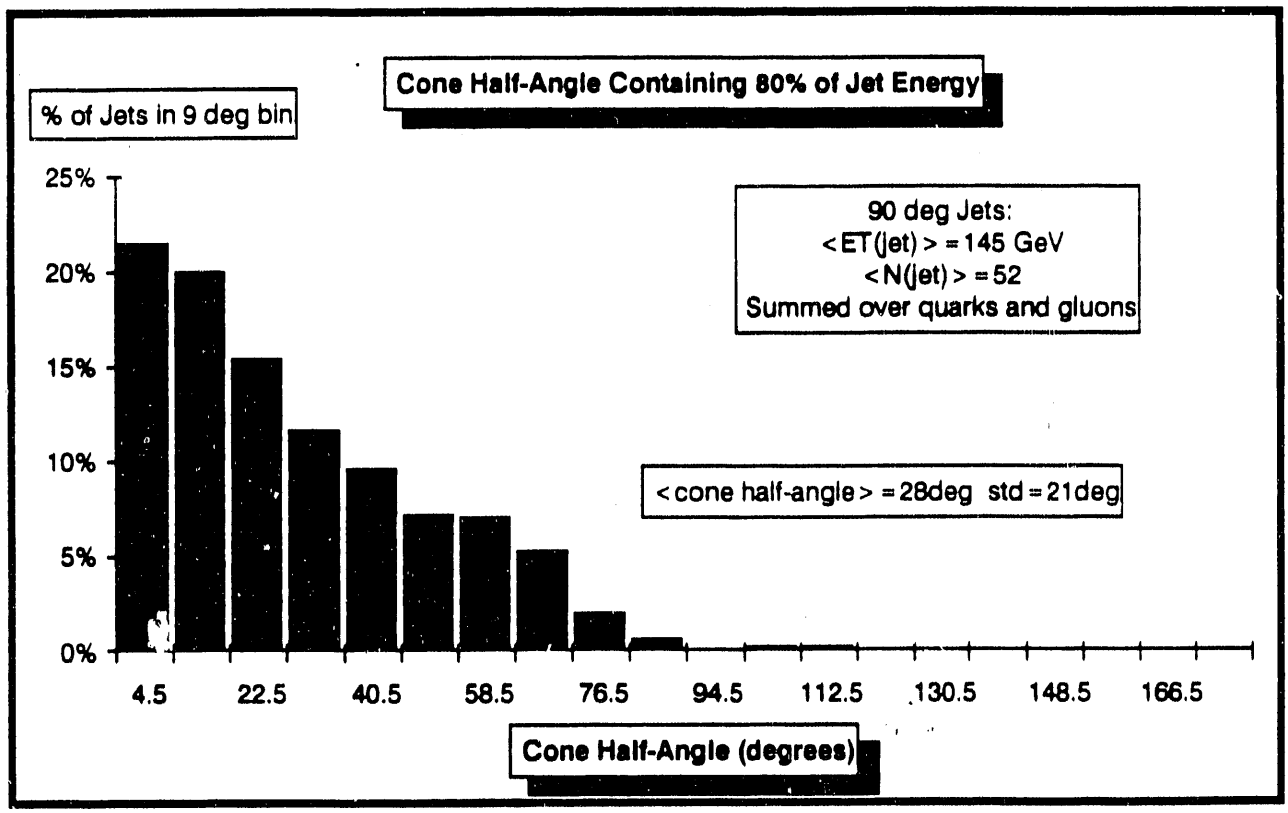
Cone Half-Angle Containing 80% of Jet Energy
% of Jets in 9 deg bin
25%
20%
15%
10%
5%
0%
90 deg Jets:
<ET(jet)> = 145 GeV
<N(jet)> = 52
Summed over quarks and gluons
<cone half-angle> = 28deg std = 21deg
4.5
22.5
40.5
58.5
76.5
94.5
112.5
130.5
148.5
166.5
Cone Half-Angle (degrees)

Figure 2

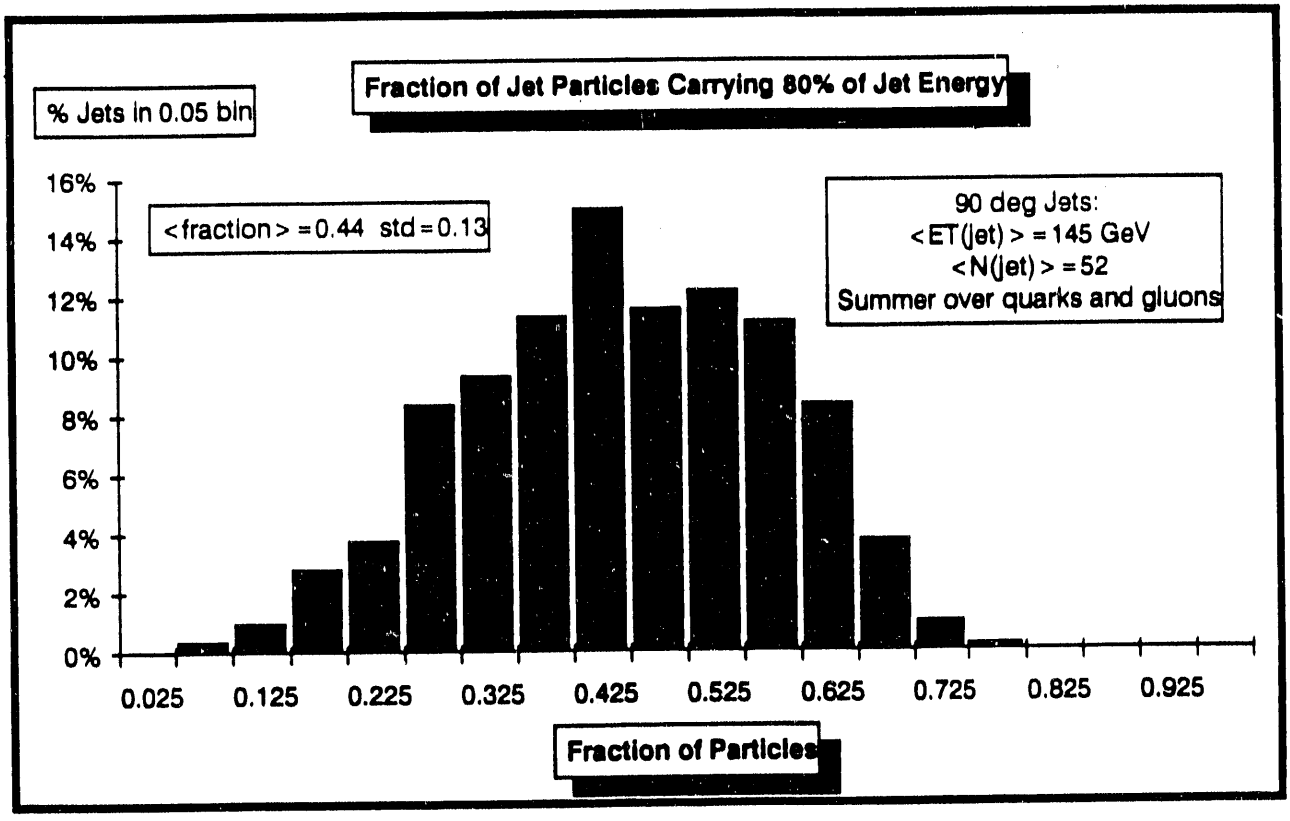
Fraction of Jet Particles Carrying 80% of Jet Energy
% Jets in 0.05 bin
<fraction> = 0.44 std = 0.13
90 deg Jets:
<ET(jet)> = 145 GeV
<N(jet)> = 52
Summer over quarks and gluons
16%
14%
12%
10%
8%
6%
4%
2%
0%
0.025
0.125
0.225
0.325
0.425
0.525
0.625
0.725
0.825
0.925
Fraction of Particles

Figure 3

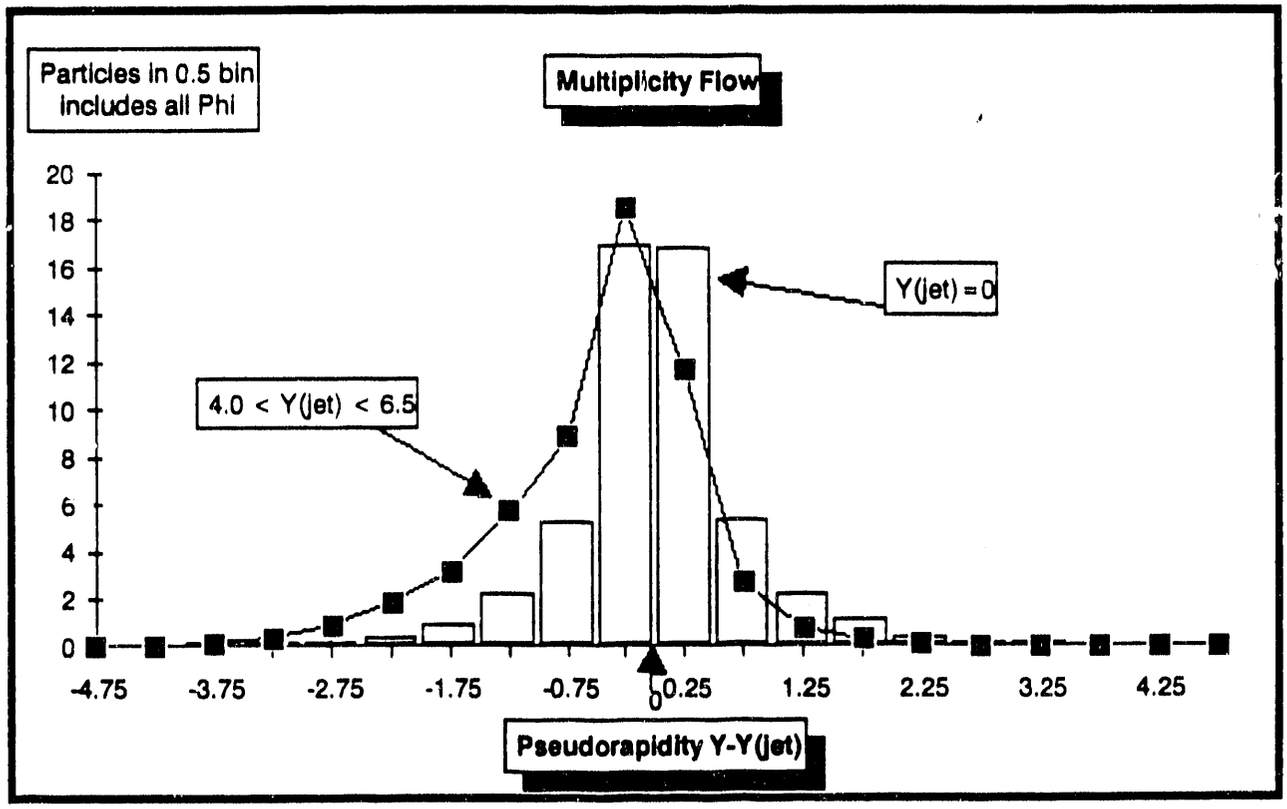
Particles in 0.5 bin
Includes all Phi
Multiplicity Flow
20
18
16
14
12
10
8
6
4
2
0
4.0 < Y(jet) < 6.5
Y(jet) = 0
-4.75
-3.75
-2.75
-1.75
-0.75
0
0.25
1.25
2.25
3.25
4.25
Pseudorapidity Y-Y(jet)

Figure 4

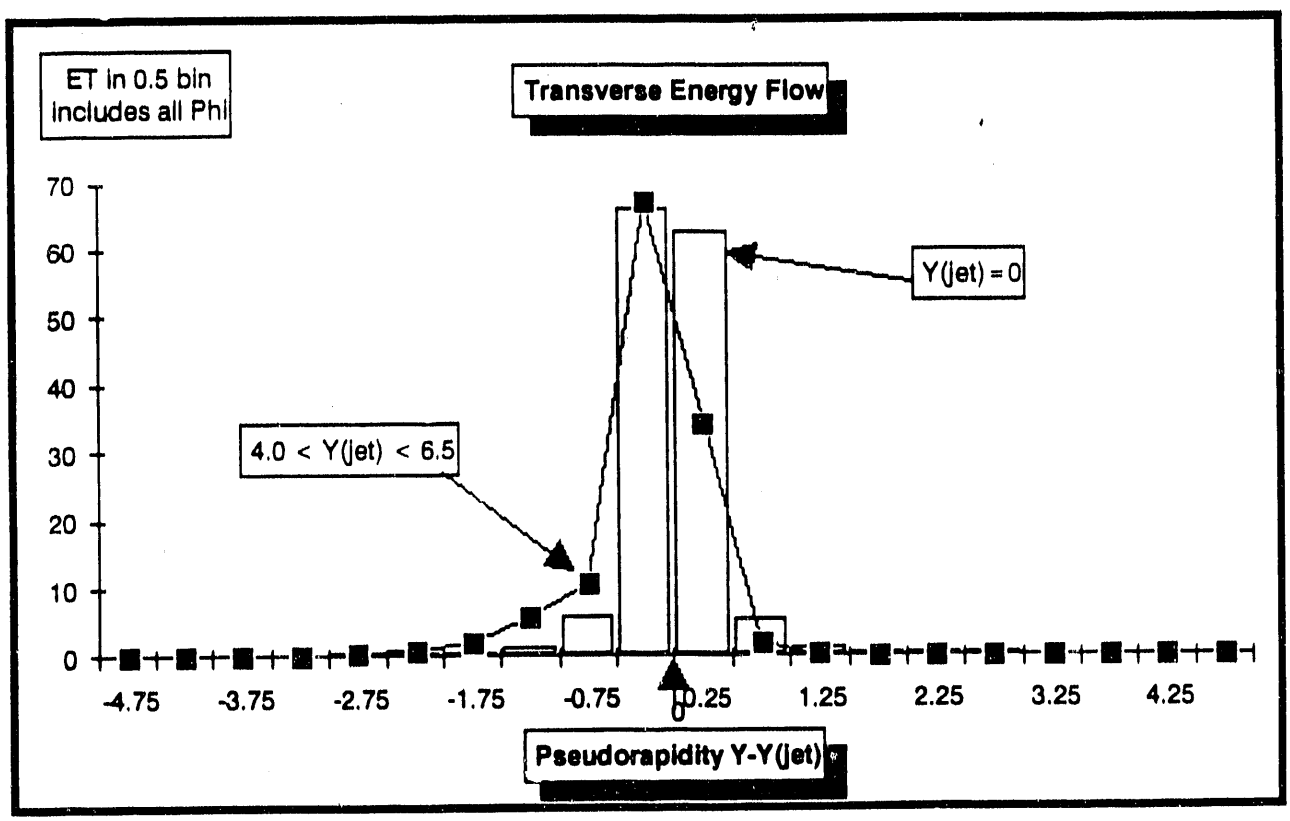
ET in 0.5 bin
includes all Phi
Transverse Energy Flow
70
60
50
40
30
20
10
0
Y(jet) = 0
4.0 < Y(jet) < 6.5
-4.75
-3.75
-2.75
-1.75
-0.75
0
0.25
1.25
2.25
3.25
4.25
Pseudorapidity Y-Y(jet)

Figure 5

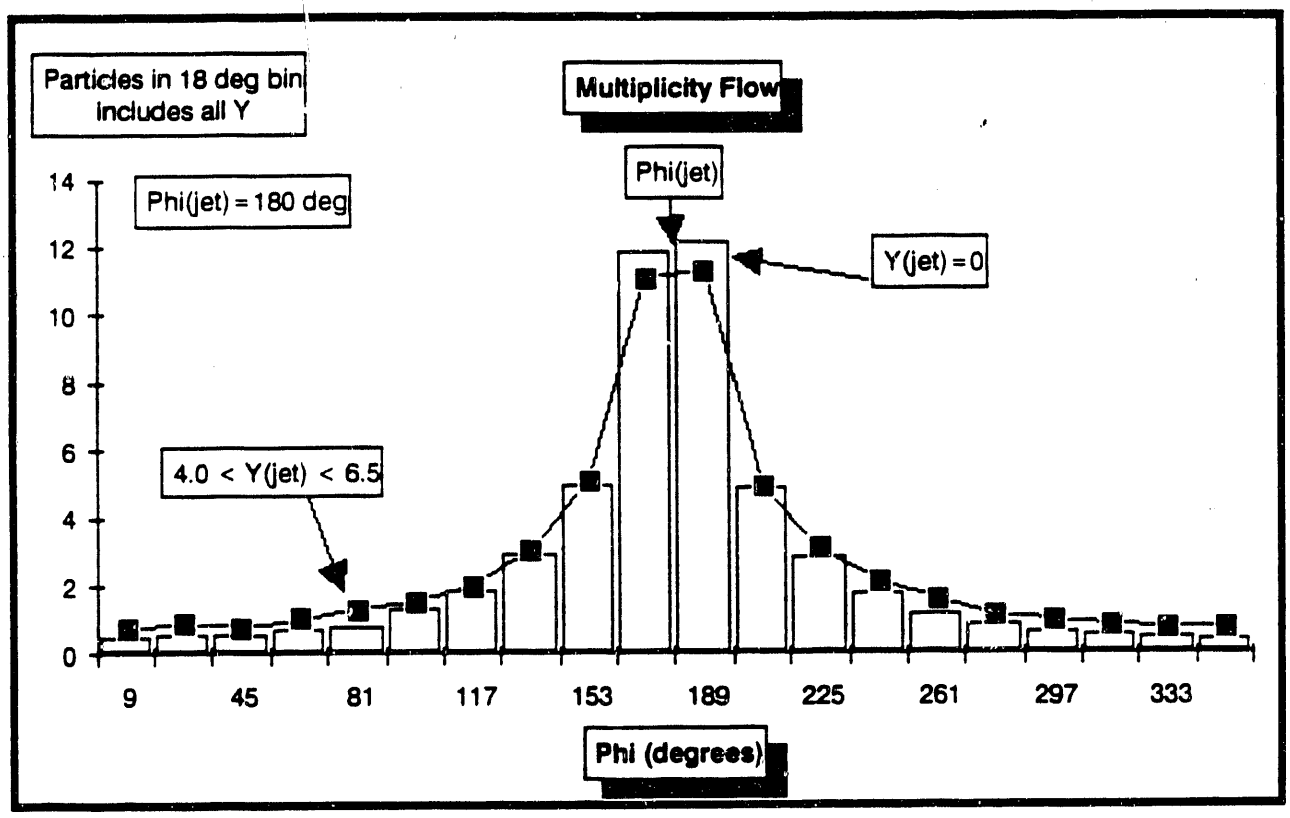
Particles in 18 deg bin
includes all Y
Multiplicity Flow
Phi(jet)
Phi(jet) = 180 deg
Y(jet) = 0
4.0 < Y(jet) < 6.5
14
12
10
8
6
4
2
0
9
45
81
117
153
189
225
261
297
333
Phi (degrees)

Figure 6

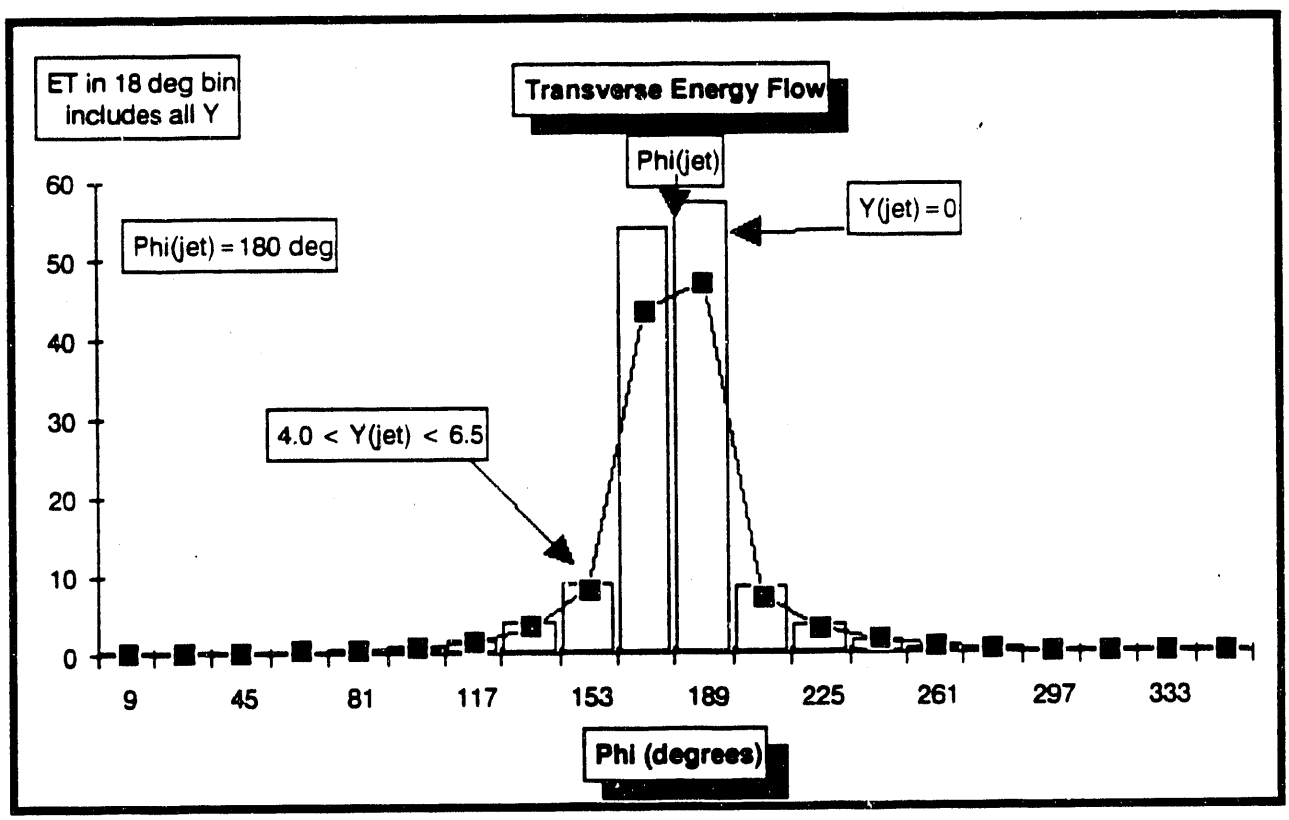
ET in 18 deg bin includes all Y
Transverse Energy Flow
Phi(jet)
Y(jet) = 0
Phi(jet) = 180 deg
4.0 < Y(jet) < 6.5
60
50
40
30
20
10
0
9
45
81
117
153
189
225
261
297
333
Phi (degrees)

Figure 7

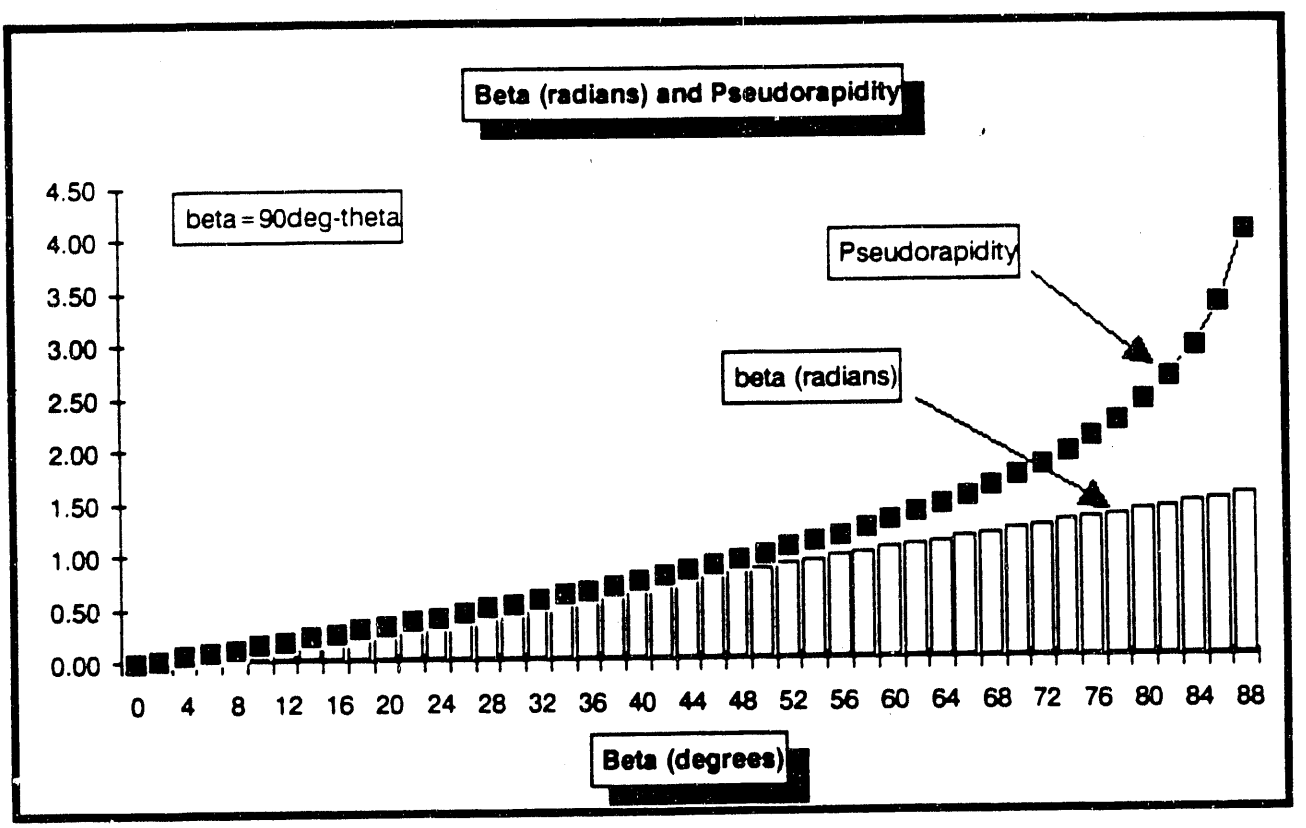
Beta (radians) and Pseudorapidity
beta = 90deg-theta
Pseudorapidity
beta (radians)
4.50
4.00
3.50
3.00
2.50
2.00
1.50
1.00
0.50
0.00
0 4 8 12 16 20 24 28 32 36 40 44 48 52 56 60 64 68 72 76 80 84 88
Beta (degrees)

Figure 8

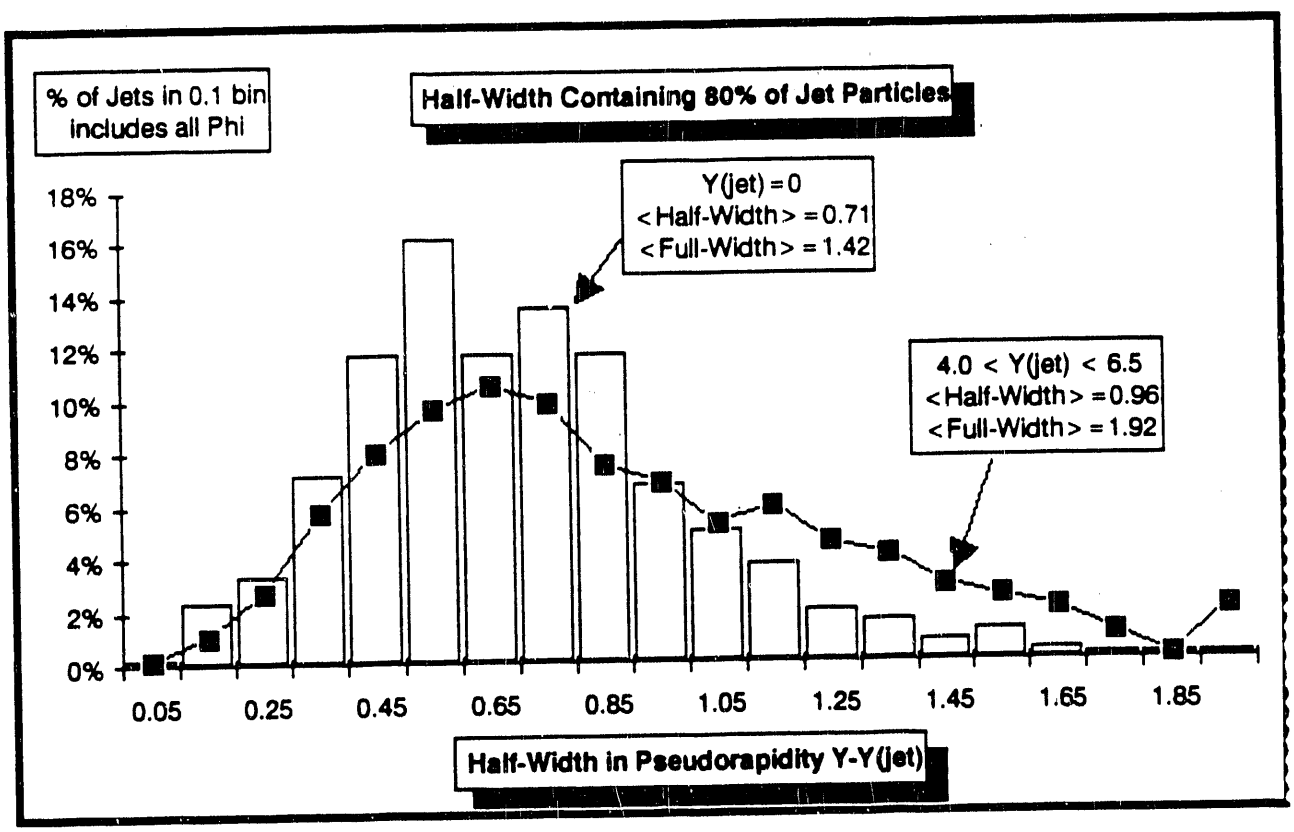
% of Jets in 0.1 bin
includes all Phi
Half-Width Containing 80% of Jet Particles
Y(jet) = 0
<Half-Width> = 0.71
<Full-Width> = 1.42
4.0 < Y(jet) < 6.5
<Half-Width> = 0.96
<Full-Width> = 1.92
18%
16%
14%
12%
10%
8%
6%
4%
2%
0%
0.05
0.25
0.45
0.65
0.85
1.05
1.25
1.45
1.65
1.85
Half-Width in Pseudorapidity Y-Y(jet)

Figure 9

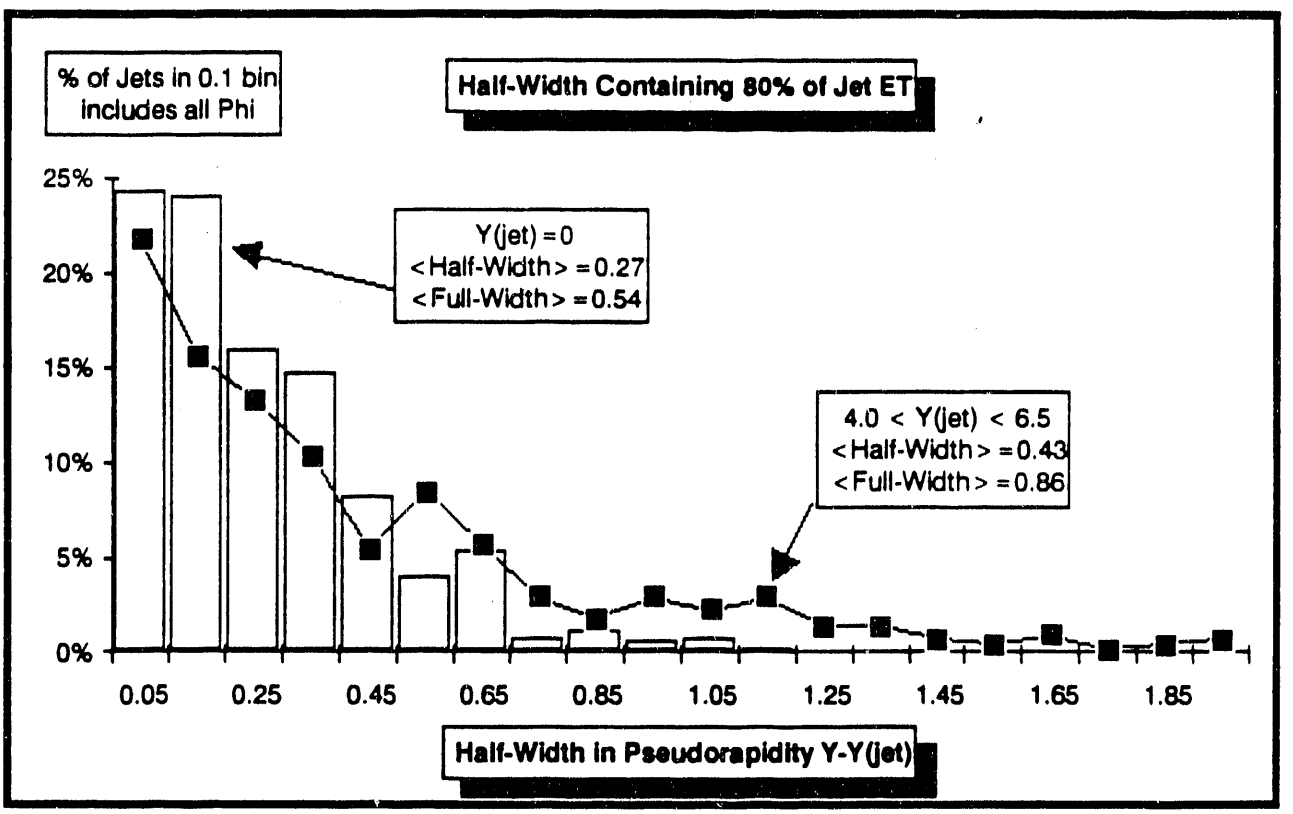
% of Jets in 0.1 bin
includes all Phi
Half-Width Containing 80% of Jet ET
25%
20%
15%
10%
5%
0%
Y(jet) = 0
<Half-Width> = 0.27
<Full-Width> = 0.54
4.0 < Y(jet) < 6.5
<Half-Width> = 0.43
<Full-Width> = 0.86
0.05
0.25
0.45
0.65
0.85
1.05
1.25
1.45
1.65
1.85
Half-Width in Pseudorapidity Y-Y(jet)

Figure 10

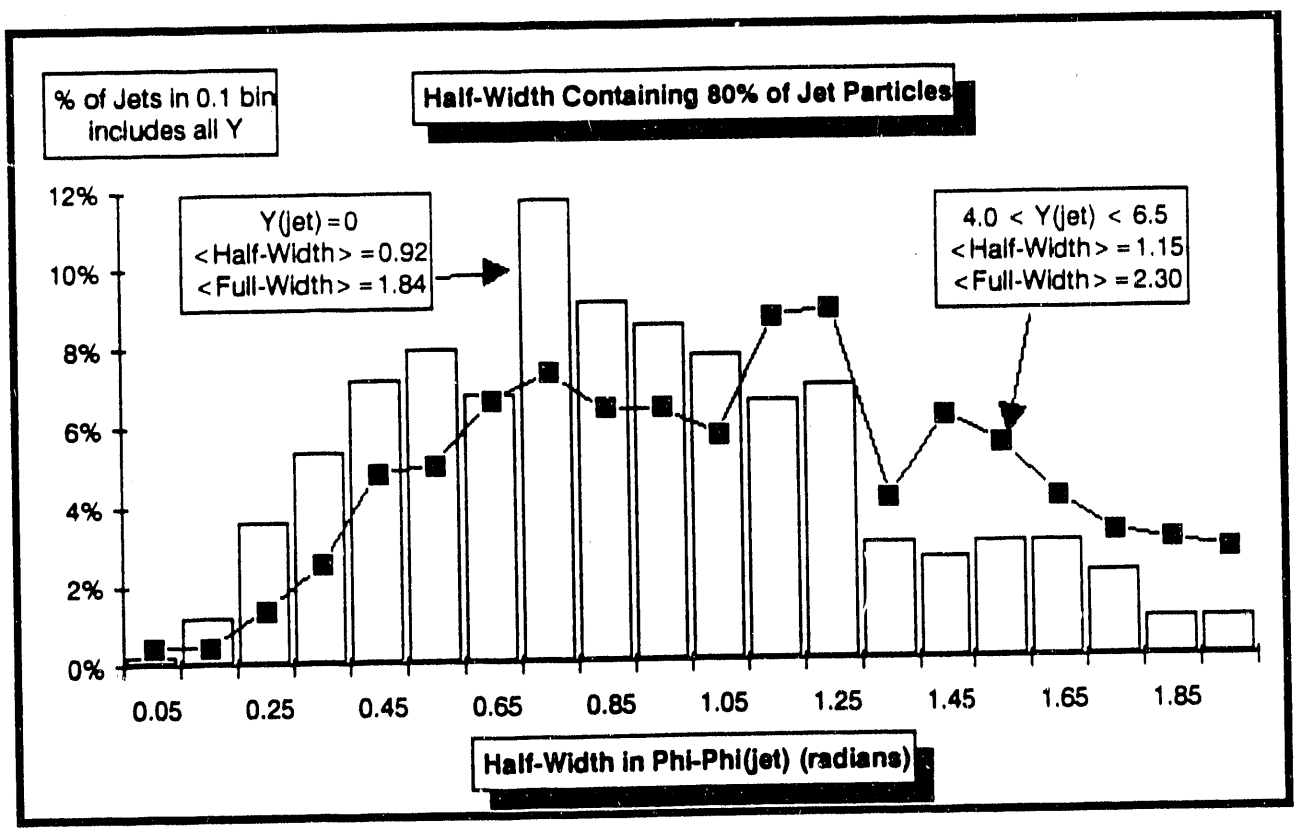
% of Jets in 0.1 bin
includes all Y
Half-Width Containing 80% of Jet Particles
12%
10%
8%
6%
4%
2%
0%
Y(jet) = 0
<Half-Width> = 0.92
<Full-Width> = 1.84
4.0 < Y(jet) < 6.5
<Half-Width> = 1.15
<Full-Width> = 2.30
0.05
0.25
0.45
0.65
0.85
1.05
1.25
1.45
1.65
1.85
Half-Width in Phi-Phi(jet) (radians)

Figure 11

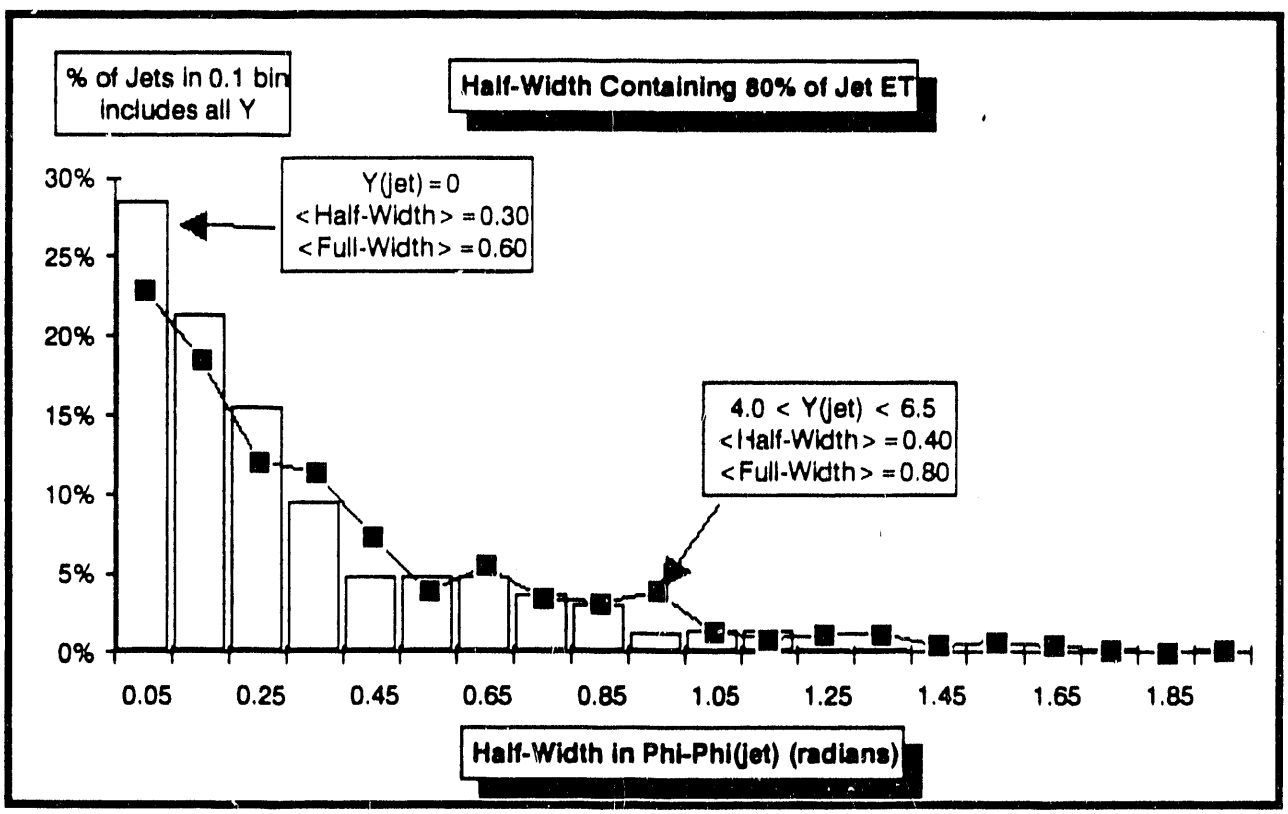
% of Jets in 0.1 bin
includes all Y
Half-Width Containing 80% of Jet ET
Y(jet) = 0
<Half-Width> = 0.30
<Full-Width> = 0.60
4.0 < Y(jet) < 6.5
<Half-Width> = 0.40
<Full-Width> = 0.80
30%
25%
20%
15%
10%
5%
0%
0.05
0.25
0.45
0.65
0.85
1.05
1.25
1.45
1.65
1.85
Half-Width in Phi-Phi(jet) (radians)

Figure 12

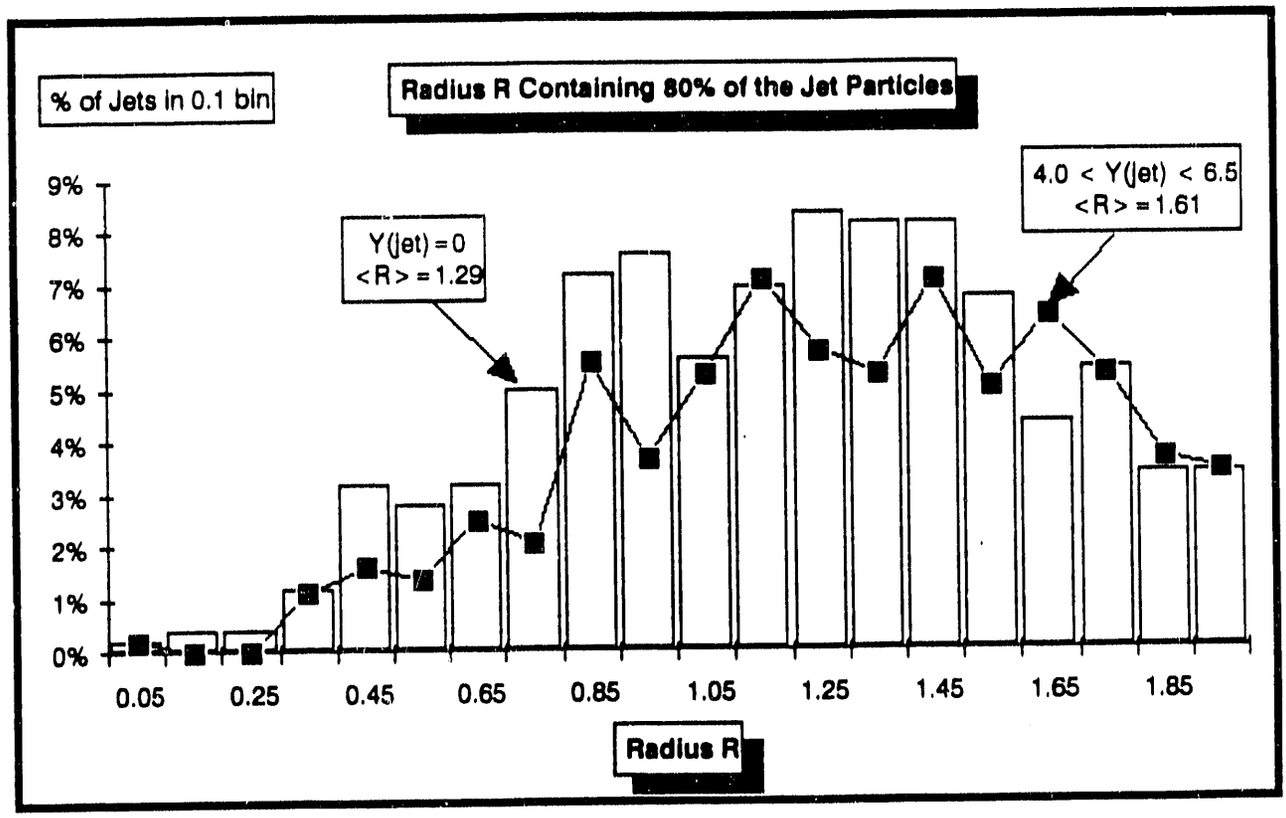
% of Jets in 0.1 bin
Radius R Containing 80% of the Jet Particles
4.0 < Y(jet) < 6.5
<R> = 1.61
Y(jet) = 0
<R> = 1.29
9%
8%
7%
6%
5%
4%
3%
2%
1%
0%
0.05
0.25
0.45
0.65
0.85
1.05
1.25
1.45
1.65
1.85
Radius R

Figure 13

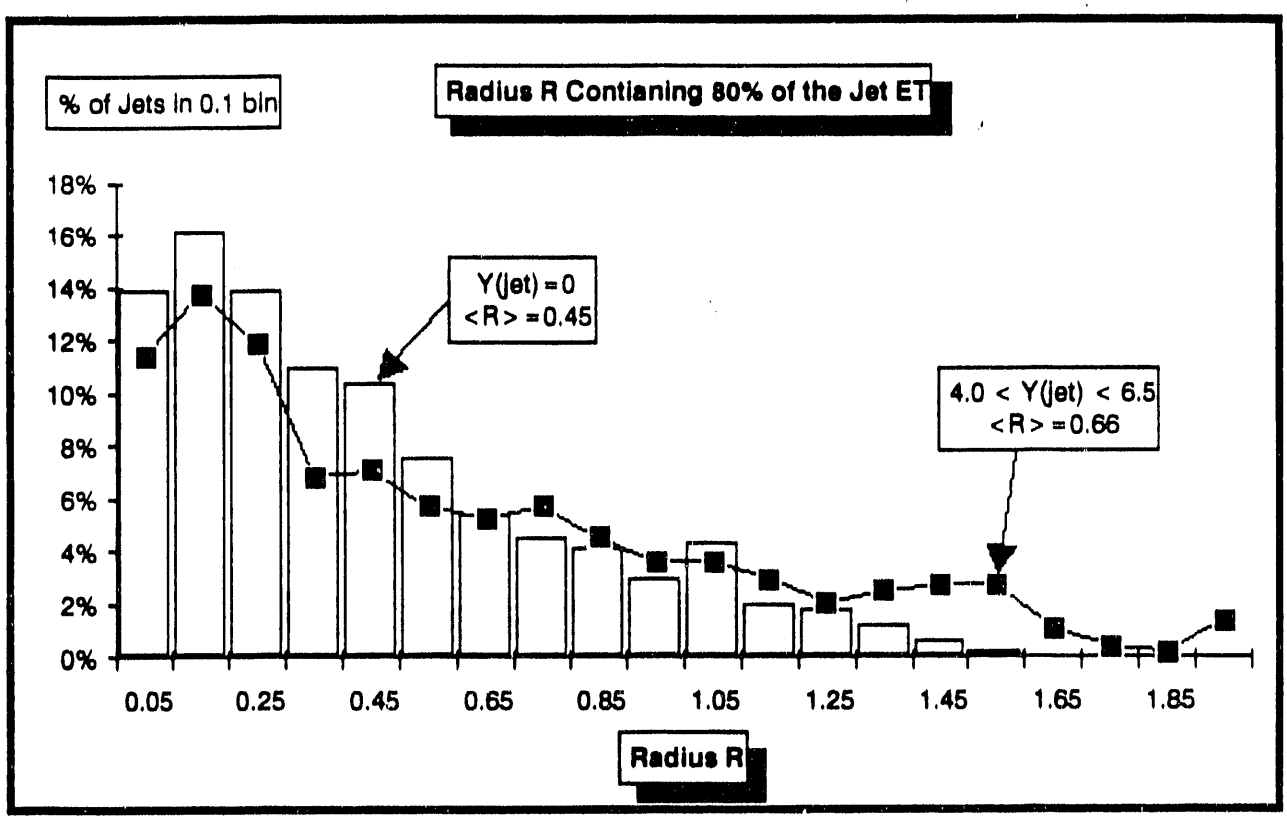
% of Jets In 0.1 bin
Radius R Contianing 80% of the Jet ET
18%
16%
14%
12%
10%
8%
6%
4%
2%
0%
Y(jet) = 0
<R> = 0.45
4.0 < Y(jet) < 6.5
<R> = 0.66
0.05
0.25
0.45
0.65
0.85
1.05
1.25
1.45
1.65
1.85
Radius R

Figure 14

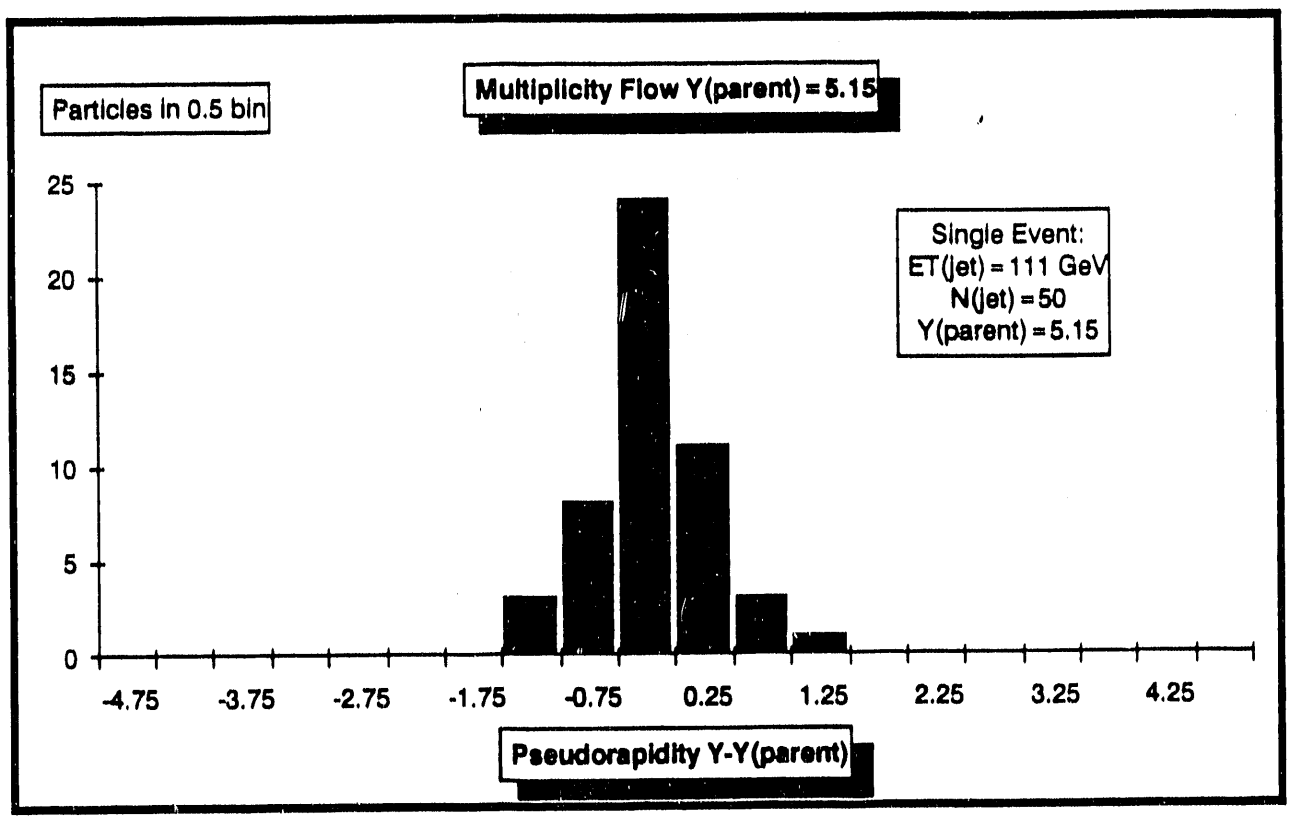
Particles in 0.5 bin
Multiplicity Flow Y(parent) = 5.15
Single Event:
ET(jet) = 111 GeV
N(jet) = 50
Y(parent) = 5.15
25
20
15
10
5
0
-4.75
-3.75
-2.75
-1.75
-0.75
0.25
1.25
2.25
3.25
4.25
Pseudorapidity Y-Y(parent)

Figure 15

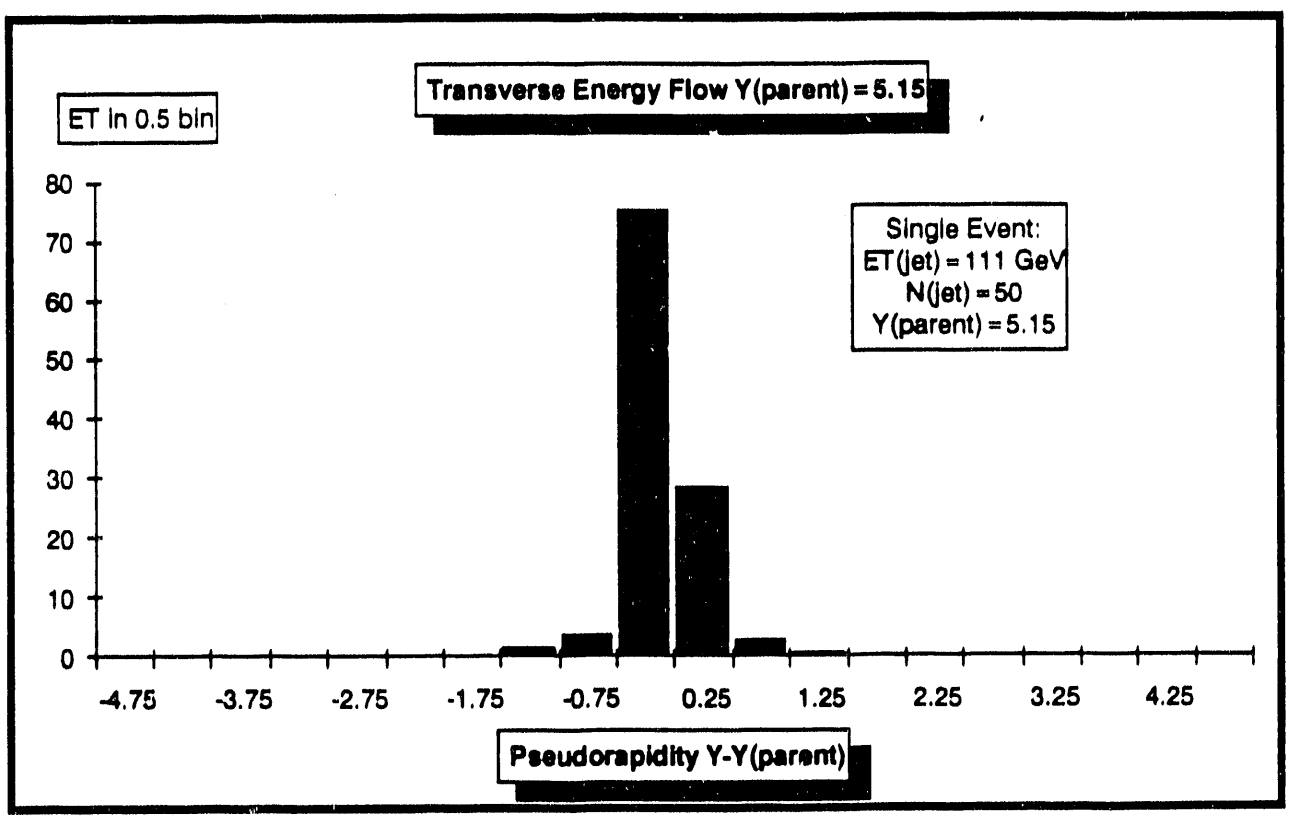
Transverse Energy Flow Y(parent) = 5.15
ET in 0.5 bin
Single Event:
ET(jet) = 111 GeV
N(jet) = 50
Y(parent) = 5.15
80
70
60
50
40
30
20
10
0
-4.75
-3.75
-2.75
-1.75
-0.75
0.25
1.25
2.25
3.25
4.25
Pseudorapidity Y-Y(parent)

Figure 16

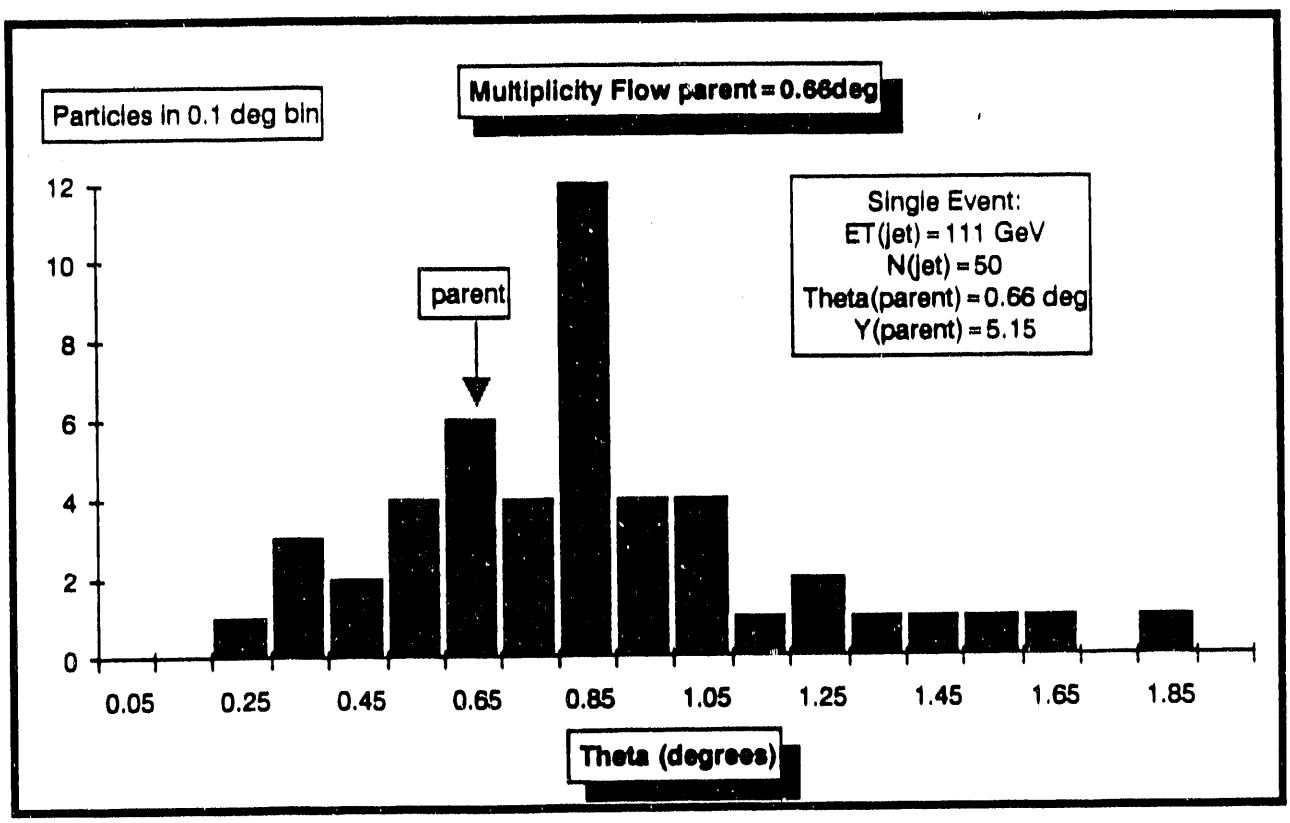
Multiplicity Flow parent = 0.66deg
Particles in 0.1 deg bin
Single Event:
ET(jet) = 111 GeV
N(jet) = 50
Theta(parent) = 0.66 deg
Y(parent) = 5.15
parent
12
10
8
6
4
2
0
0.05
0.25
0.45
0.65
0.85
1.05
1.25
1.45
1.65
1.85
Theta (degrees)

Figure 17

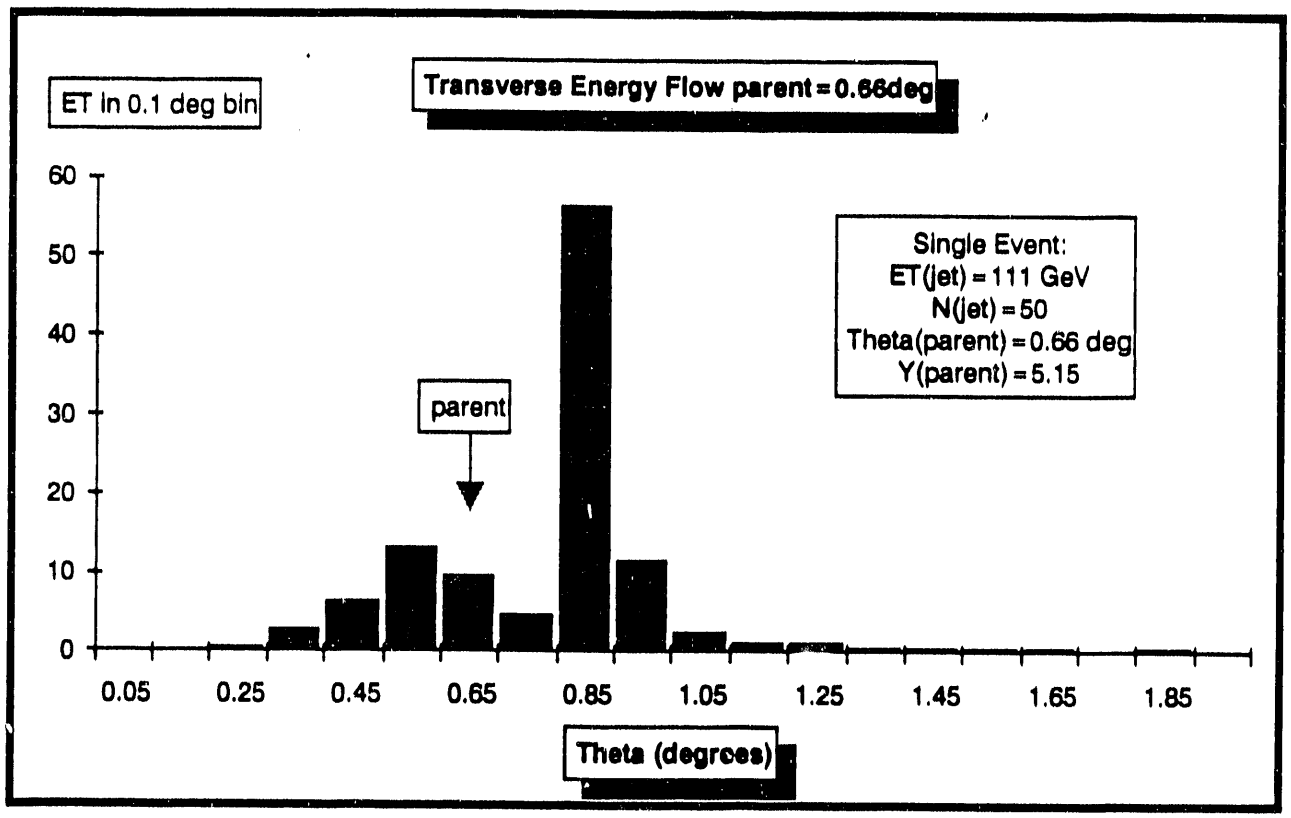
ET in 0.1 deg bin
Transverse Energy Flow parent = 0.66deg
60
50
40
30
20
10
0
parent
Single Event:
ET(jet) = 111 GeV
N(jet) = 50
Theta(parent) = 0.66 deg
Y(parent) = 5.15
0.05
0.25
0.45
0.65
0.85
1.05
1.25
1.45
1.65
1.85
Theta (degrees)

Figure 18

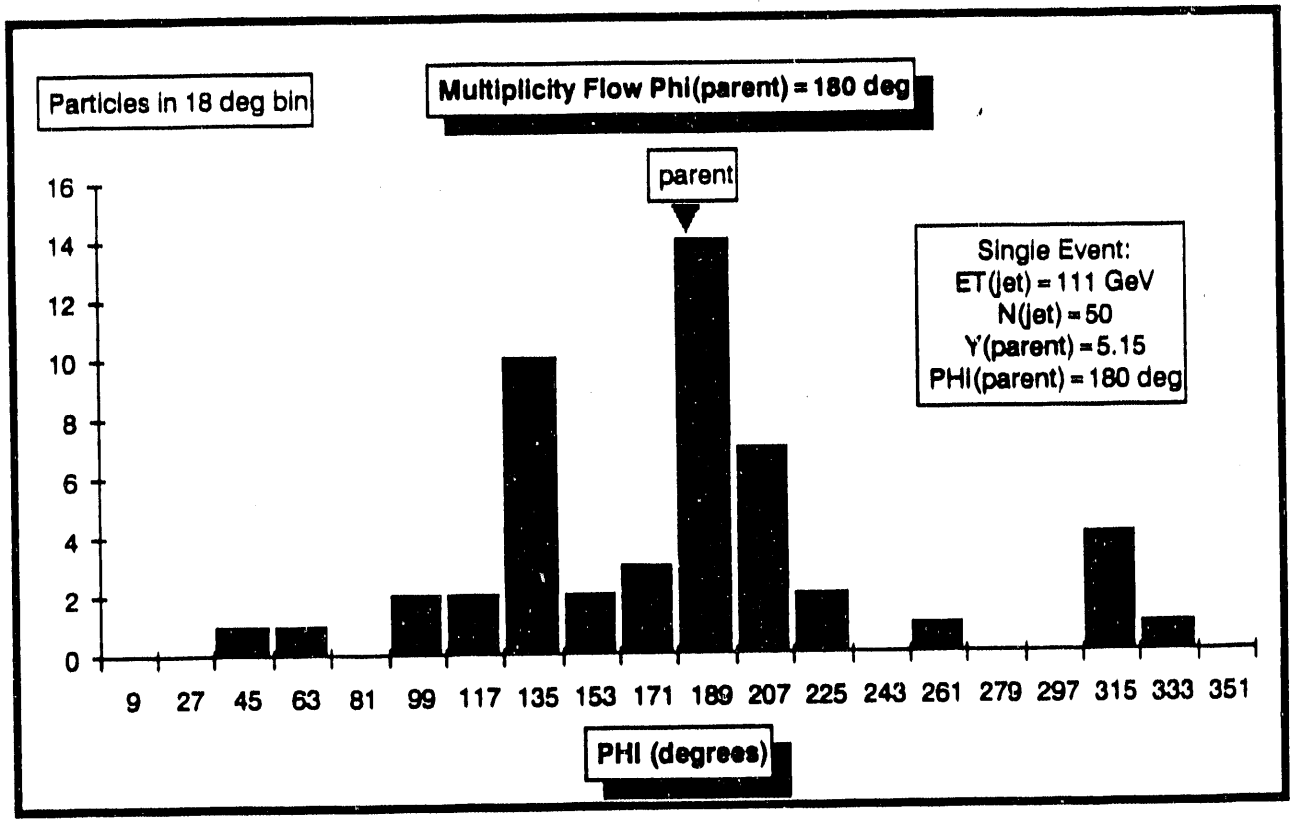
Particles in 18 deg bin
Multiplicity Flow Phi(parent) = 180 deg
parent
Single Event:
ET(jet) = 111 GeV
N(jet) = 50
Y(parent) = 5.15
PHI(parent) = 180 deg
16
14
12
10
8
6
4
2
0
9 27 45 63 81 99 117 135 153 171 189 207 225 243 261 279 297 315 333 351
PHI (degrees)

Figure 19

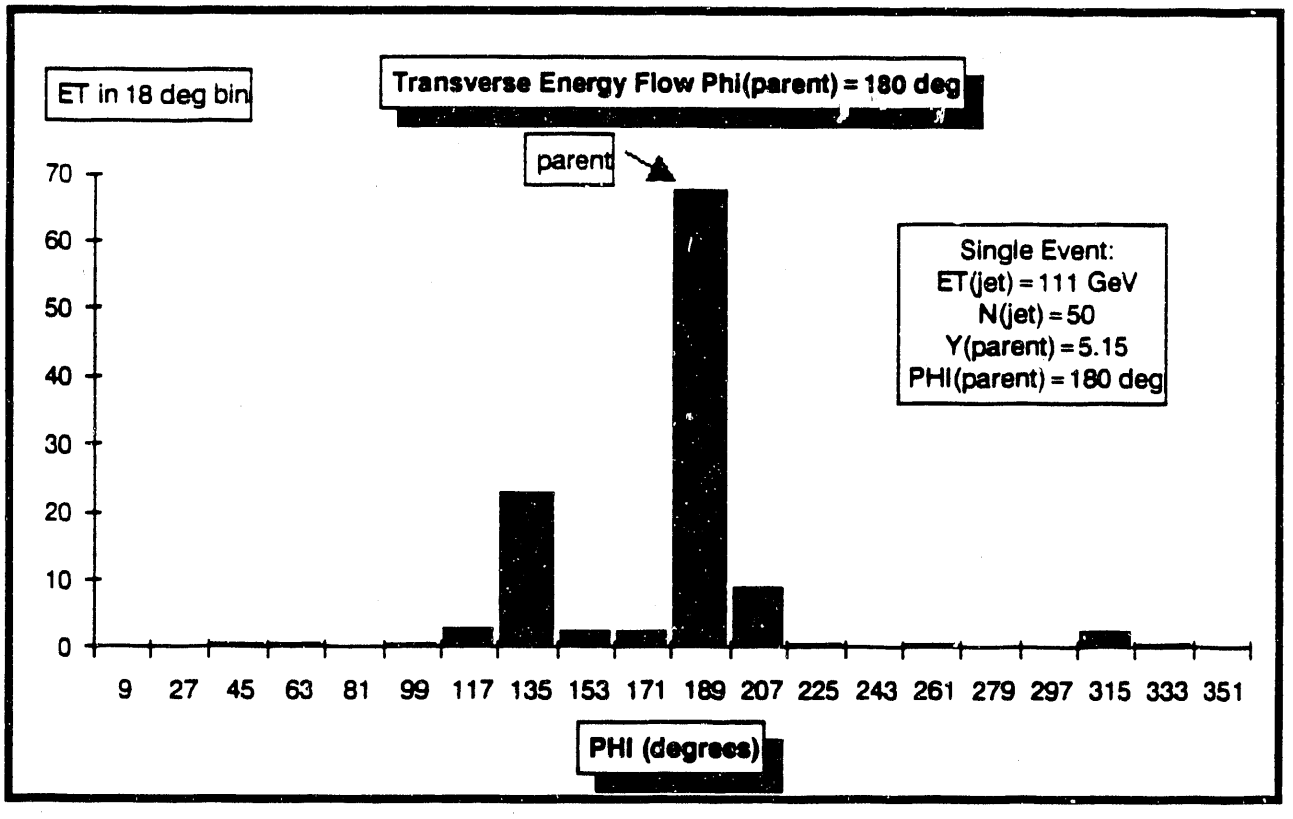
ET in 18 deg bin
Transverse Energy Flow Phi(parent) = 180 deg
parent
Single Event:
ET(jet) = 111 GeV
N(jet) = 50
Y(parent) = 5.15
PHI(parent) = 180 deg
70
60
50
40
30
20
10
0
9 27 45 63 81 99 117 135 153 171 189 207 225 243 261 279 297 315 333 351
PHI (degrees)

Figure 20

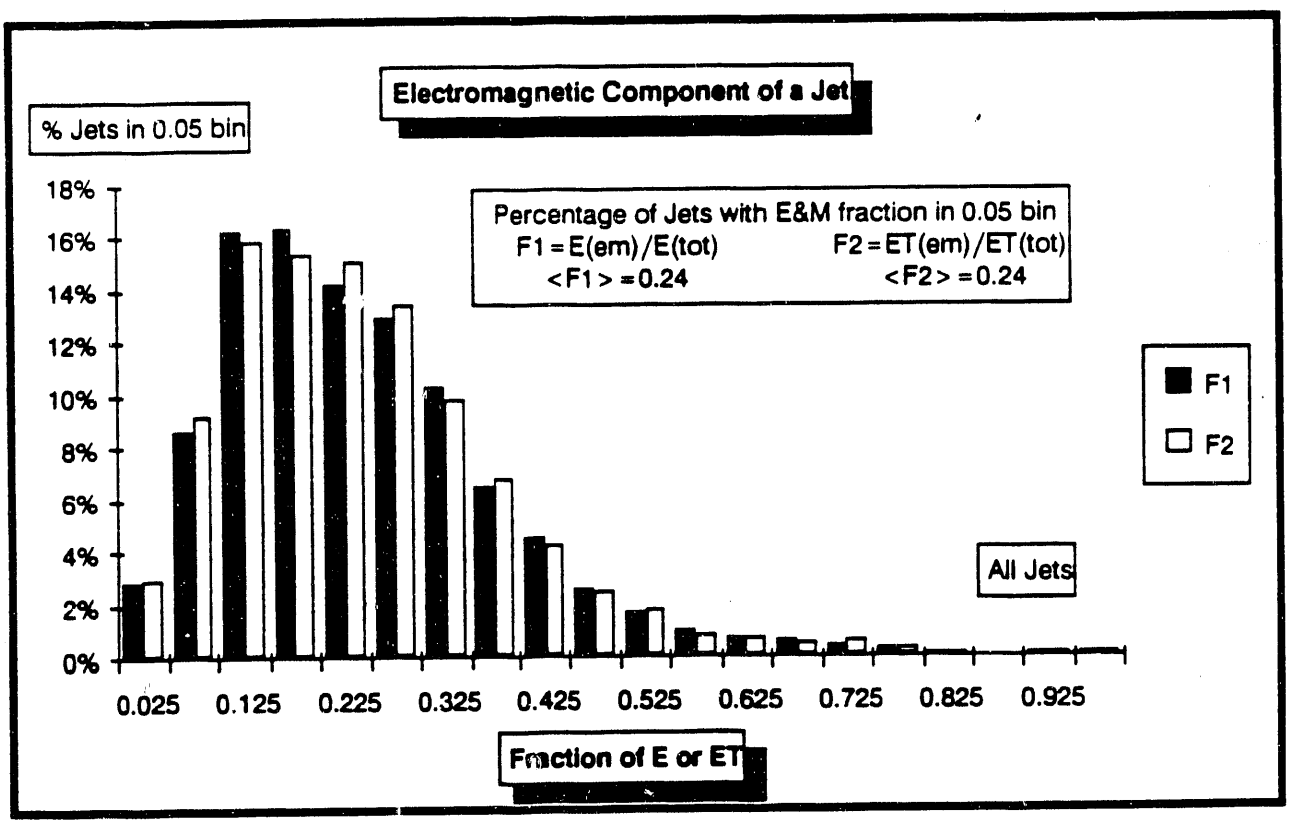
Electromagnetic Component of a Jet
% Jets in 0.05 bin
Percentage of Jets with E&M fraction in 0.05 bin
F1 = E(em)/E(tot)
<F1> = 0.24
F2 = ET(em)/ET(tot)
<F2> = 0.24
F1
F2
All Jets
18%
16%
14%
12%
10%
8%
6%
4%
2%
0%
0.025
0.125
0.225
0.325
0.425
0.525
0.625
0.725
0.825
0.925
Fraction of E or ET

Figure 21

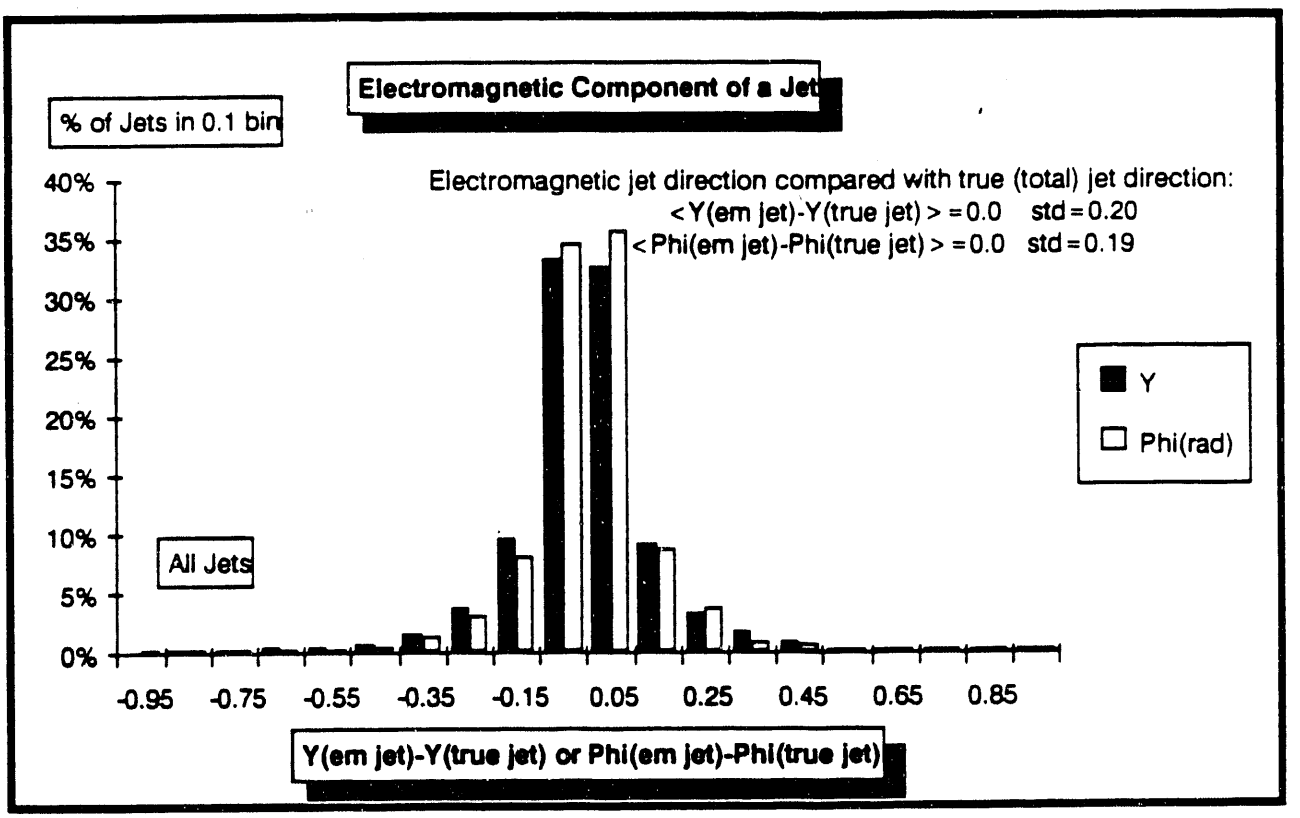
Electromagnetic Component of a Jet
% of Jets in 0.1 bin
Electromagnetic jet direction compared with true (total) jet direction:
<Y(em jet)-Y(true jet)> = 0.0 std = 0.20
<Phi(em jet)-Phi(true jet)> = 0.0 std = 0.19
40%
35%
30%
25%
20%
15%
10%
5%
0%
Y
Phi(rad)
All Jets
-0.95
-0.75
-0.55
-0.35
-0.15
0.05
0.25
0.45
0.65
0.85
Y(em jet)-Y(true jet) or Phi(em jet)-Phi(true jet)

Figure 22

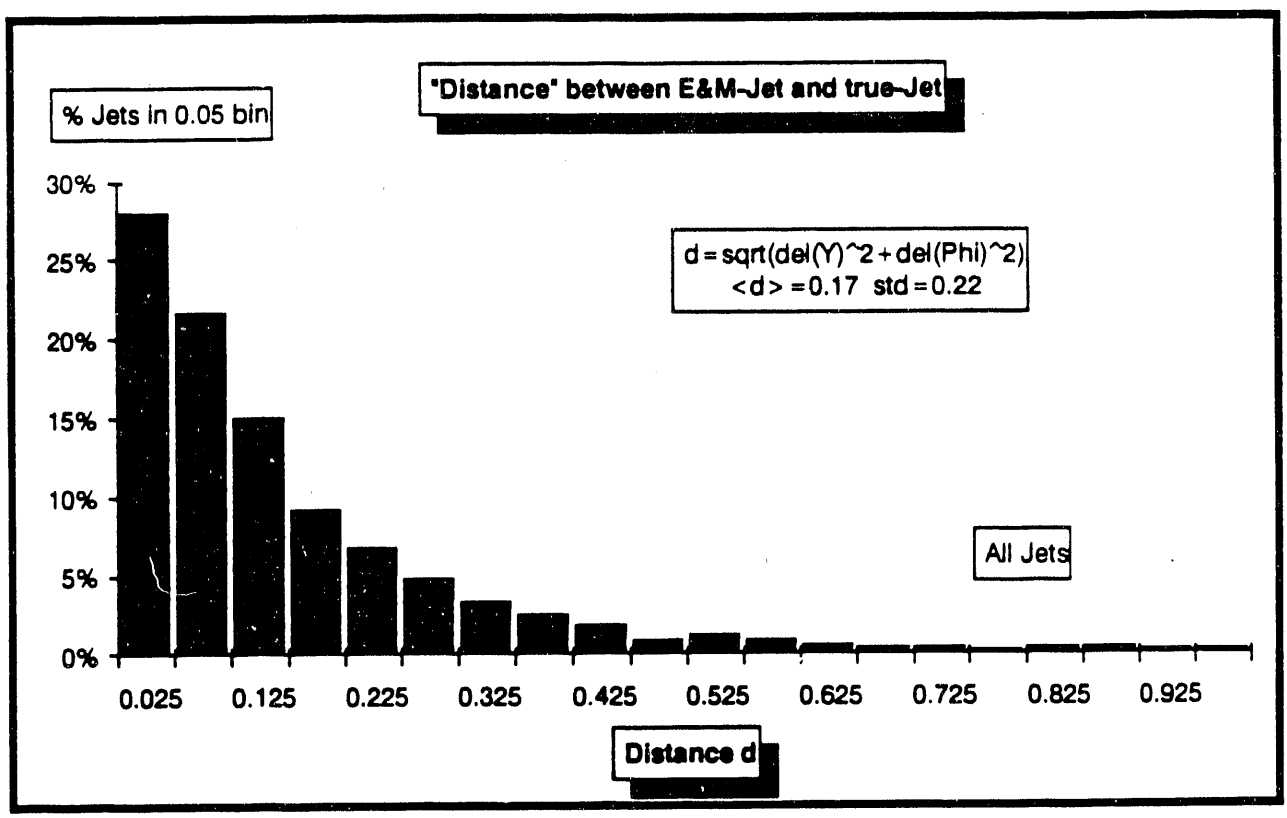
"Distance" between E&M-Jet and true-Jet
% Jets in 0.05 bin
d = sqrt(del(Y)^2 + del(Phi)^2)
<d> = 0.17 std = 0.22
All Jets
30%
25%
20%
15%
10%
5%
0%
0.025
0.125
0.225
0.325
0.425
0.525
0.625
0.725
0.825
0.925
Distance d

Figure 23

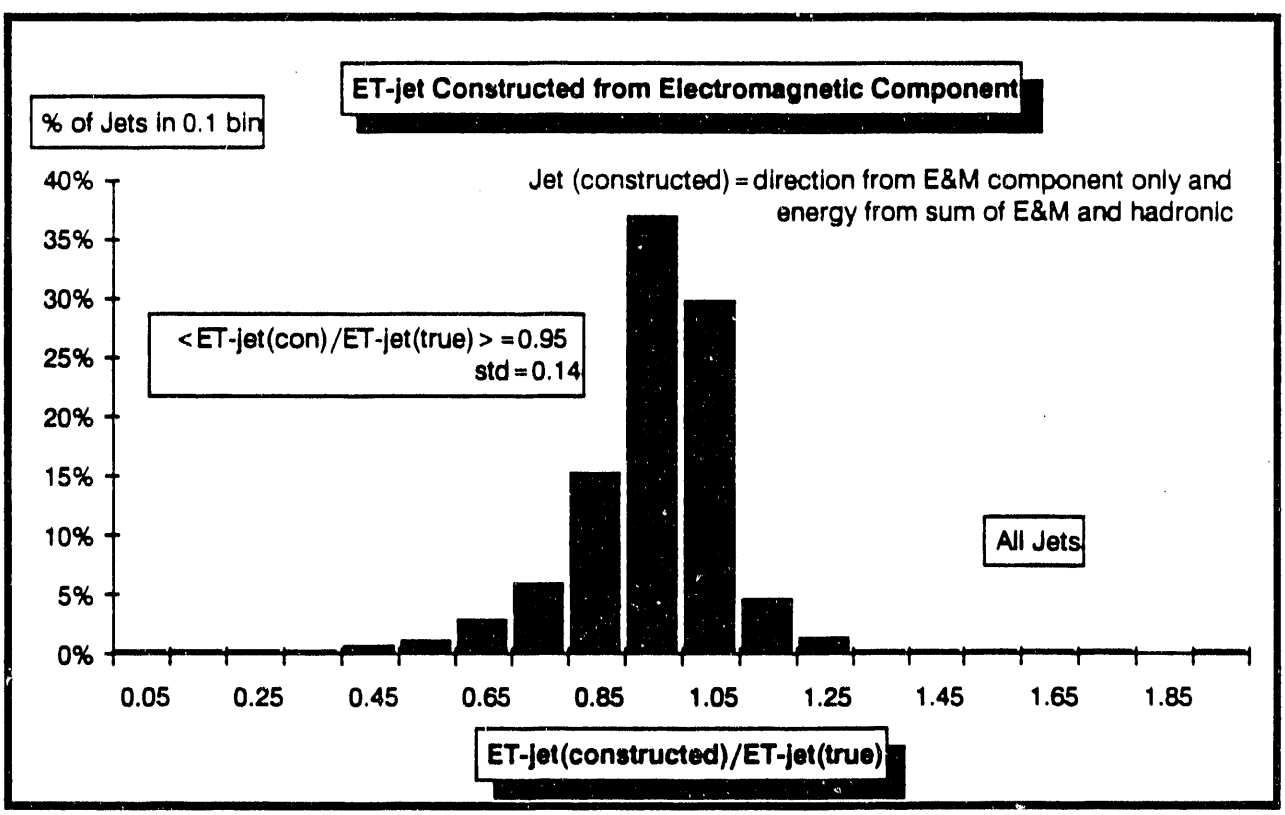
ET-jet Constructed from Electromagnetic Component
% of Jets in 0.1 bin
Jet (constructed) = direction from E&M component only and energy from sum of E&M and hadronic
<ET-jet(con)/ET-jet(true)> = 0.95
std = 0.14
All Jets
40%
35%
30%
25%
20%
15%
10%
5%
0%
0.05
0.25
0.45
0.65
0.85
1.05
1.25
1.45
1.65
1.85
ET-jet(constructed)/ET-jet(true)

Figure 24

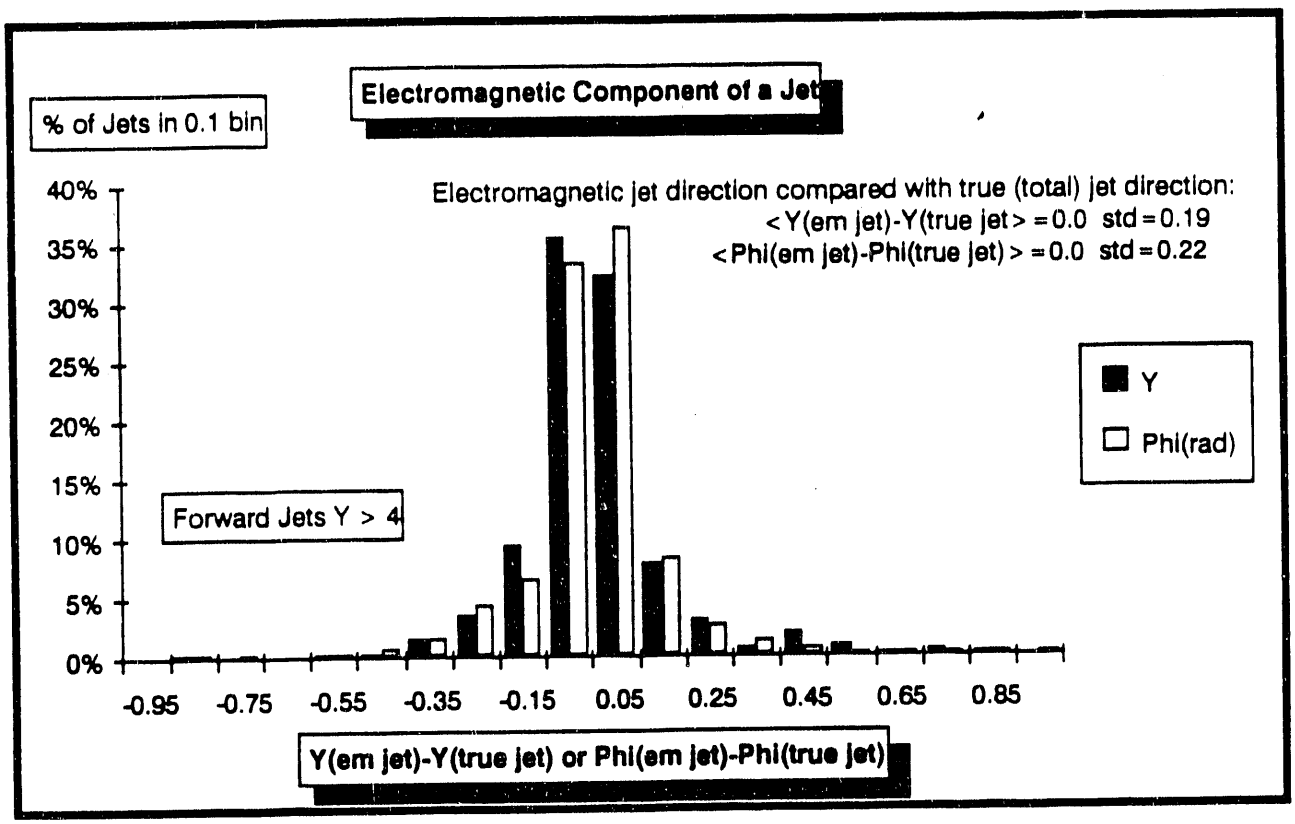
Electromagnetic Component of a Jet
% of Jets in 0.1 bin
Electromagnetic jet direction compared with true (total) jet direction:
<Y(em jet)-Y(true jet> =0.0 std=0.19
<Phi(em jet)-Phi(true jet)> =0.0 std=0.22
40%
35%
30%
25%
20%
15%
10%
5%
0%
Y
Phi(rad)
Forward Jets Y > 4
-0.95
-0.75
-0.55
-0.35
-0.15
0.05
0.25
0.45
0.65
0.85
Y(em jet)-Y(true jet) or Phi(em jet)-Phi(true jet)

Figure 25

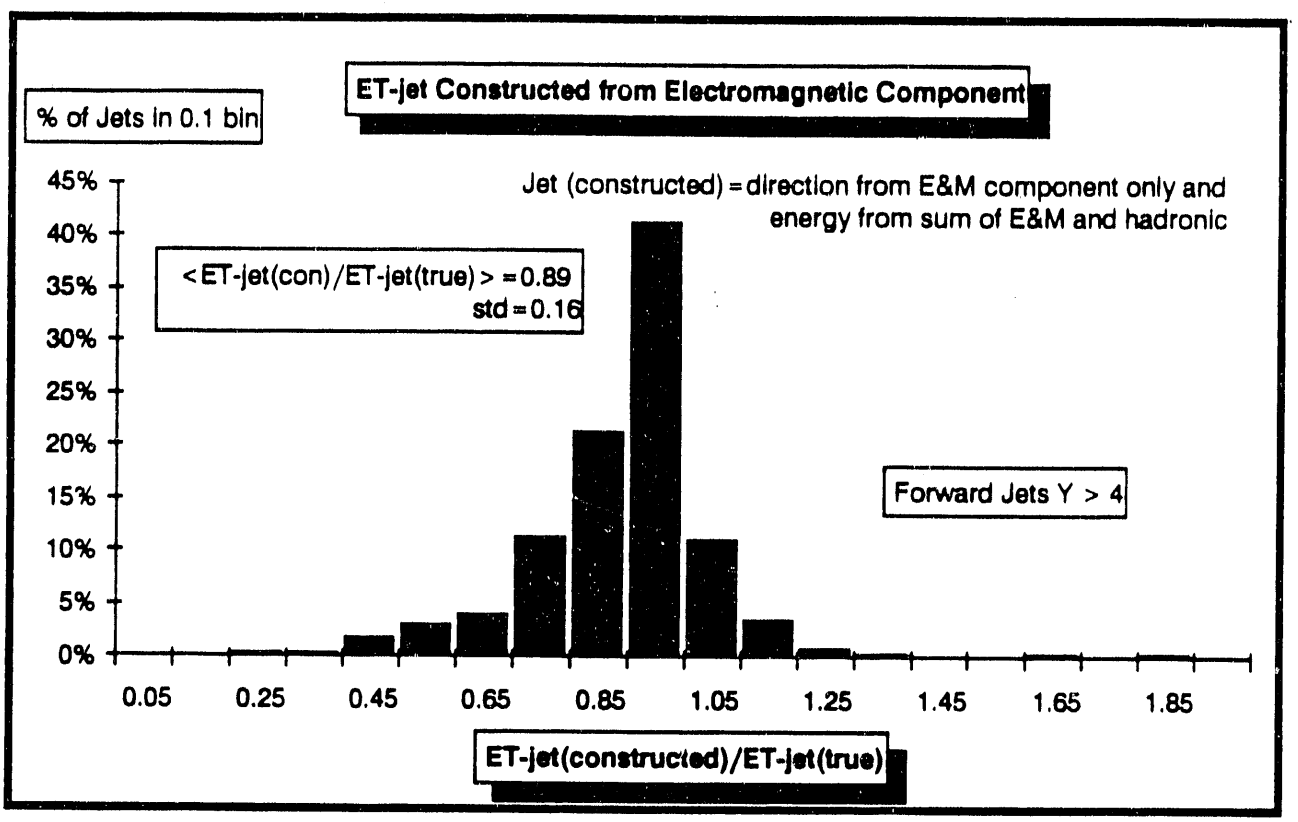
ET-jet Constructed from Electromagnetic Component
% of Jets in 0.1 bin
Jet (constructed) = direction from E&M component only and energy from sum of E&M and hadronic
<ET-jet(con)/ET-jet(true)> = 0.89
std = 0.16
Forward Jets Y > 4
45%
40%
35%
30%
25%
20%
15%
10%
5%
0%
0.05
0.25
0.45
0.65
0.85
1.05
1.25
1.45
1.65
1.85
ET-jet(constructed)/ET-jet(true)

Figure 26

END

DATE FILMED

4/15/92